(2)

REPORT DOCUMENTATION PAGE

Form Approved
OMB No. 0704-0188

1. AGENCY USE ONLY (Leave blank)	2. REPORT DATE	3. REPORT TYPE AND DATES COVERED
		Final Report/15 Nov 88-14 Nov 89

4. TITLE AND SUBTITLE

Multiple Optical Probing of High Frequency Semiconductor Devices

5. FUNDING NUMBERS

61104D/3842/A6

6. AUTHOR(S)

Harold Fetterman

7. PERFORMING ORGANIZATION NAME(S) AND ADDRESS(ES)

University of California
Dept of Electrical Engineering
Los Angeles, CA 90024

8. PERFORMING ORGANIZATION REPORT NUMBER

AFOSR-TR- 90 1129

9. SPONSORING/MONITORING AGENCY NAME(S) AND ADDRESS(ES)

AFOSR/NP
Bolling AFB DC 20332-6448

10. SPONSORING/MONITORING AGENCY REPORT NUMBER

AFOSR-89-0111

11. SUPPLEMENTARY NOTES

12a. DISTRIBUTION/AVAILABILITY STATEMENT

Approved for public release; distribution is unlimited.

12b. DISTRIBUTION CODE

13. ABSTRACT *(Maximum 200 words)*

This grant was a Defense University Research Instrumentation Program (DURIP) and the university purchased a complete Nd: YAG pumped picosecond dye laser and related optical components. The university then provided matching support for an autocorrelator, power meters, lock-in detectors and Optical Table to form a complete measurement system.

14. SUBJECT TERMS	15. NUMBER OF PAGES
picosecond, dye, laser, measurement, system	47
	16. PRICE CODE: UL

17. SECURITY CLASSIFICATION OF REPORT	18. SECURITY CLASSIFICATION OF THIS PAGE	19. SECURITY CLASSIFICATION OF ABSTRACT	20. LIMITATION OF ABSTRACT
UNCLASSIFIED	UNCLASSIFIED	UNCLASSIFIED	SAR

FINAL REPORT AFOSR - 89 - 0111

MULTIPLE OPTICAL PROBING

OF HIGH FREQUENCY

SEMICONDUCTOR DEVICES

This effort is based upon the purchase of a complete Nd: YAG pumped picosecond dye laser and related optical components. ~~The university then provided~~ matching support for an autocorrelator, power meters, lock-in detectors and Optical Table to form a complete measurement system. The idea was to fabricate a picosecond system which would measure devices and systems out to at least 200 GHz. It would be used to validate ~~our~~ Network analyzer measurements in the region of overlap, ~~but was also~~ to develop a degree of confidence in the entire technique of "S" parameter measurement using picosecond pulses.

In addition to investigating the highest frequency GaAs and GaAs alloy devices, ~~we also planned to study~~ new types of devices, MMIC amplifiers and finally the operational constraits of optical interconnections. The system proved to be so useful that we actually performed all of these tests and have extended these measurements to the generation of millimeter radiation and the demonstration of spectroscopic

use. Our current measurements are on ballistic field effect devices and resonant tunneling structures which have been fabricated by local industries and universities directly as a result of this unique measurement capability.

CONFIGURATION

The basic system used is shown in figure 1 and simply uses optical delays generated by a mirror stepping motor system. In figure 2 we see the basic Auston switch arrangement used in most of our measurements. We also used slightly modified sample mounts when we had amplifiers with multiple bias connections and more recently when we have looked at cooled systems including superconducting devices. In some cases we also illuminated the devices directly and used them as phototransistors.

MEASUREMENTS

Our first work was on Heterojunction Bipolar transistors which had only been fully characterized to 26 GHz. This work was on the first generation of these devices. Again, we are continuing these measurement today with

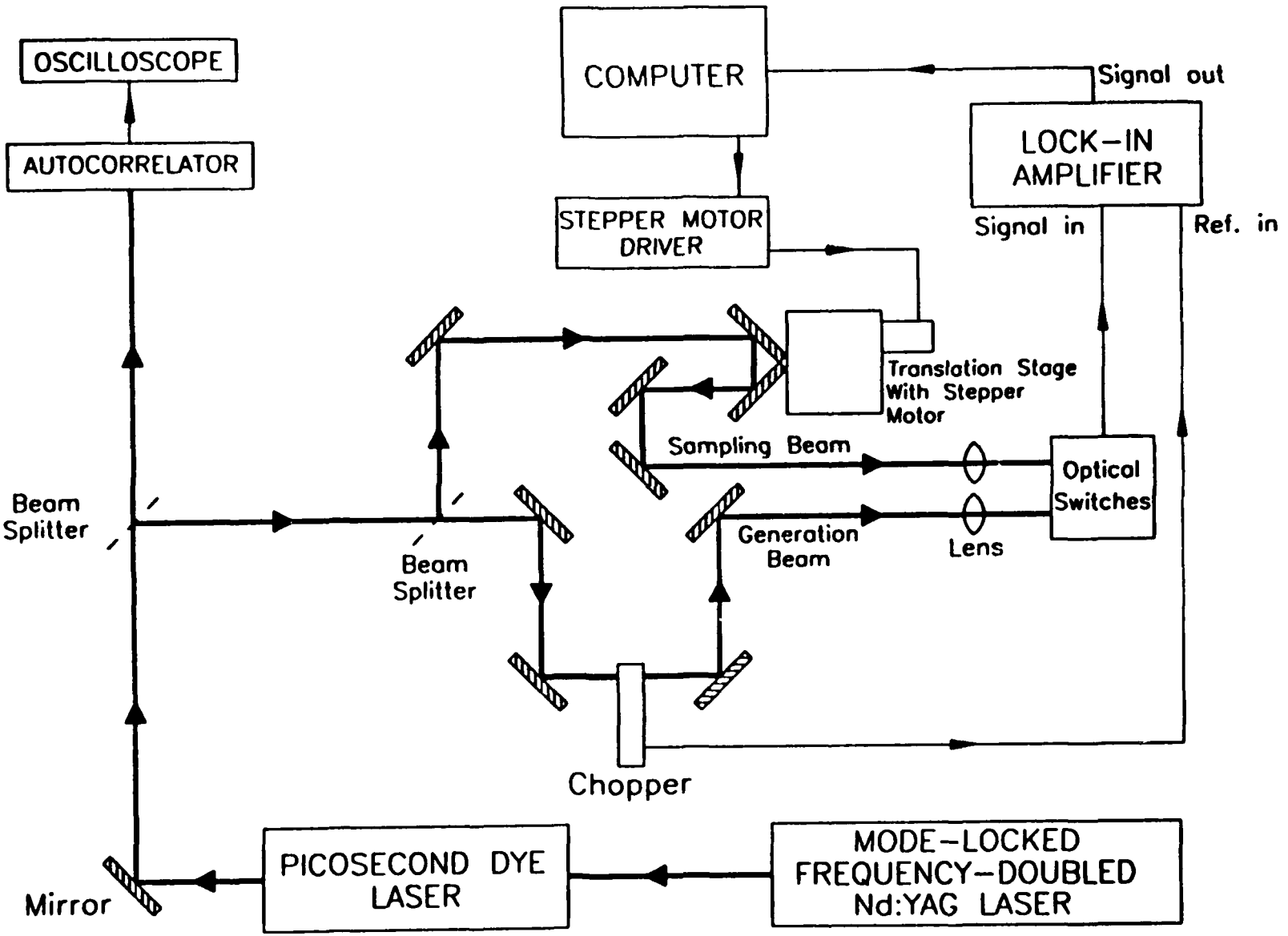
OSCILLOSCOPE
AUTOCORRELATOR
COMPUTER
Signal out
LOCK–IN AMPLIFIER
STEPPER MOTOR DRIVER
Signal in
Ref. in
Translation Stage With Stepper Motor
Sampling Beam
Optical Switches
Beam Splitter
Beam Splitter
Generation Beam
Lens
Chopper
Mirror
PICOSECOND DYE LASER
MODE–LOCKED FREQUENCY–DOUBLED Nd:YAG LASER

Figure 1

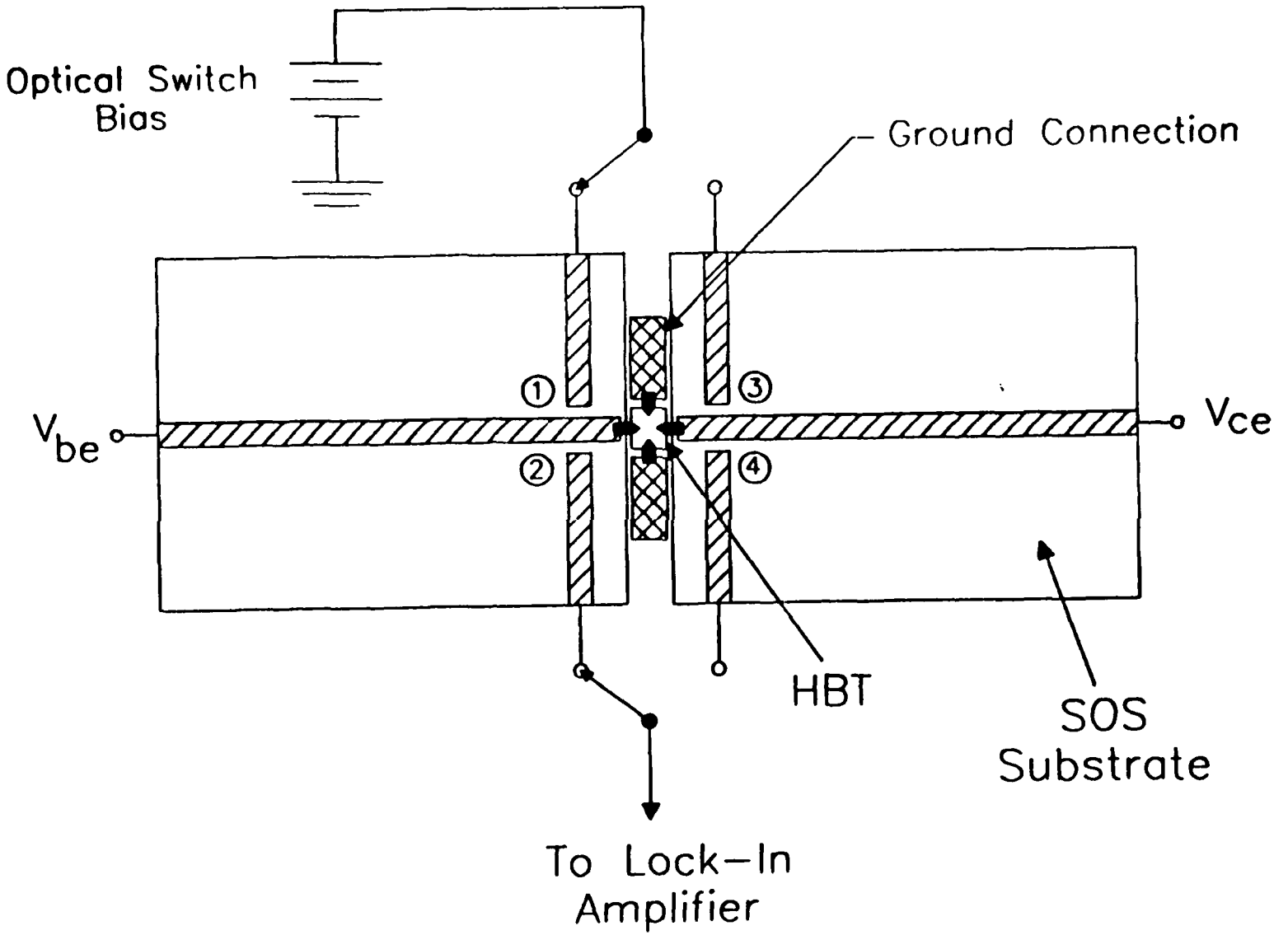
Optical Switch
Bias
Ground Connection
①
②
③
④
V_{be}
V_{ce}
HBT
SOS
Substrate
To Lock-In
Amplifier

Figure 2

devices which go above 100 GHz. These measurements are included in the first paper attached. The actual results of forward transmission of the picosecond sampling system we used is shown in figure 3. Taking the Transform the "S" parameters can be plotted as shown in figure 4. In the same figure the crosses show the results of electrical measurements.

Subsequently we measured MMIC devices as shown in figure 5. On this same figure we see the measurements that were made electrically and which were limited to 26 GHz. High resolution measurement were made up to 50 Ghz. and are shown in figures 6a and 6b. The next step was to measure higher frequency devices and try to validate them electrically. In Figure 7 we show the measurement made on a high frequency HEMT device. The actual paper is included as paper #2. and shows the complete measurement of "S" parameters. For some of the measurements there is a problem with the reference plane of the phase. However, in virtually all the cases where the electrical measurements differed from the optical the problem was found to be in the electrical ones.

Lastly, we used the laser to generate high energy picosecond electrical pulses in an FET. Using a twin dipole integrated antenna we radiated this power and detected it in a similar system as shown in figure 8. The pulse comb at 60

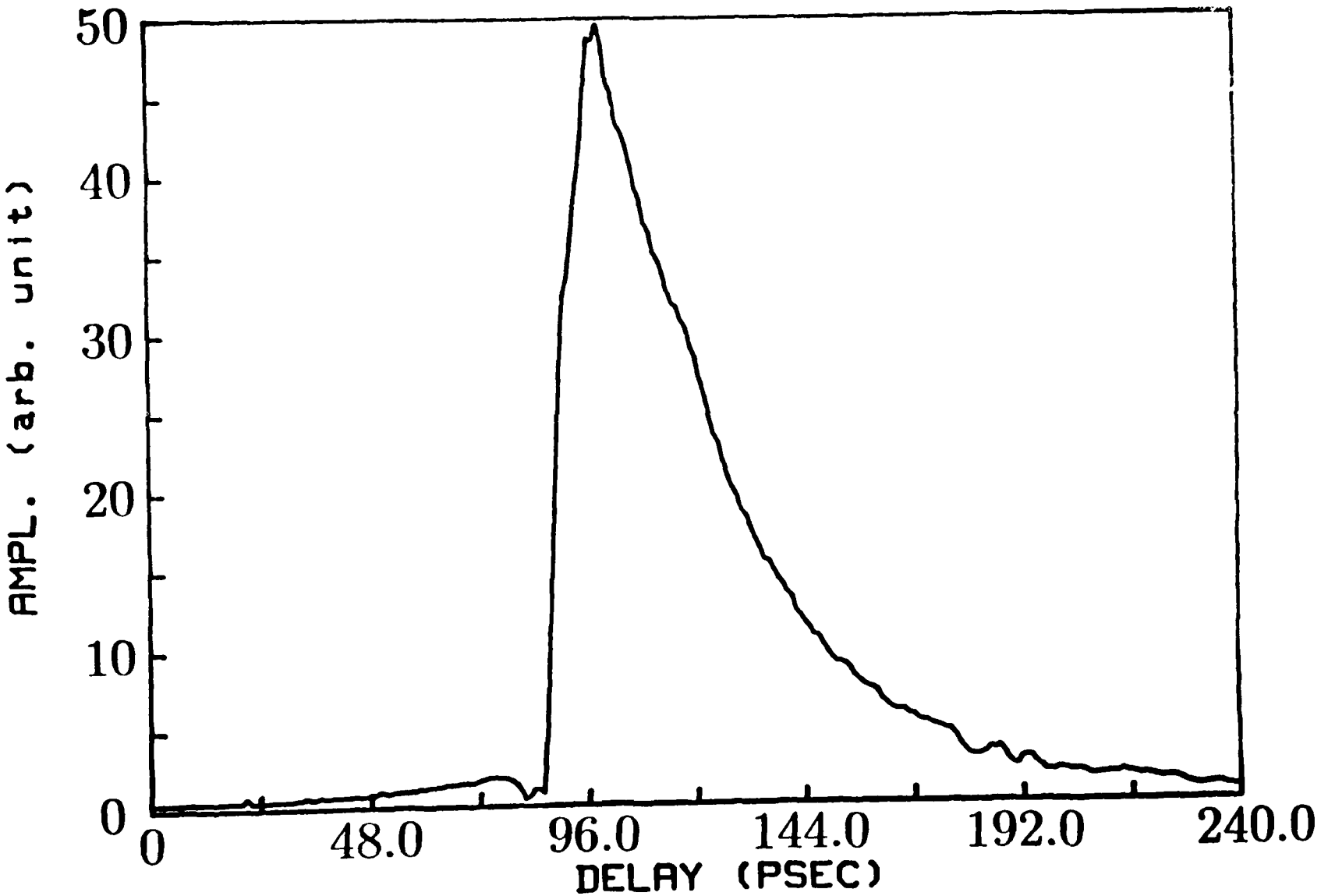
50
40
30
20
10
0
AMPL. (arb. unit)
0
48.0
96.0
144.0
192.0
240.0
DELAY (PSEC)

Figure 3

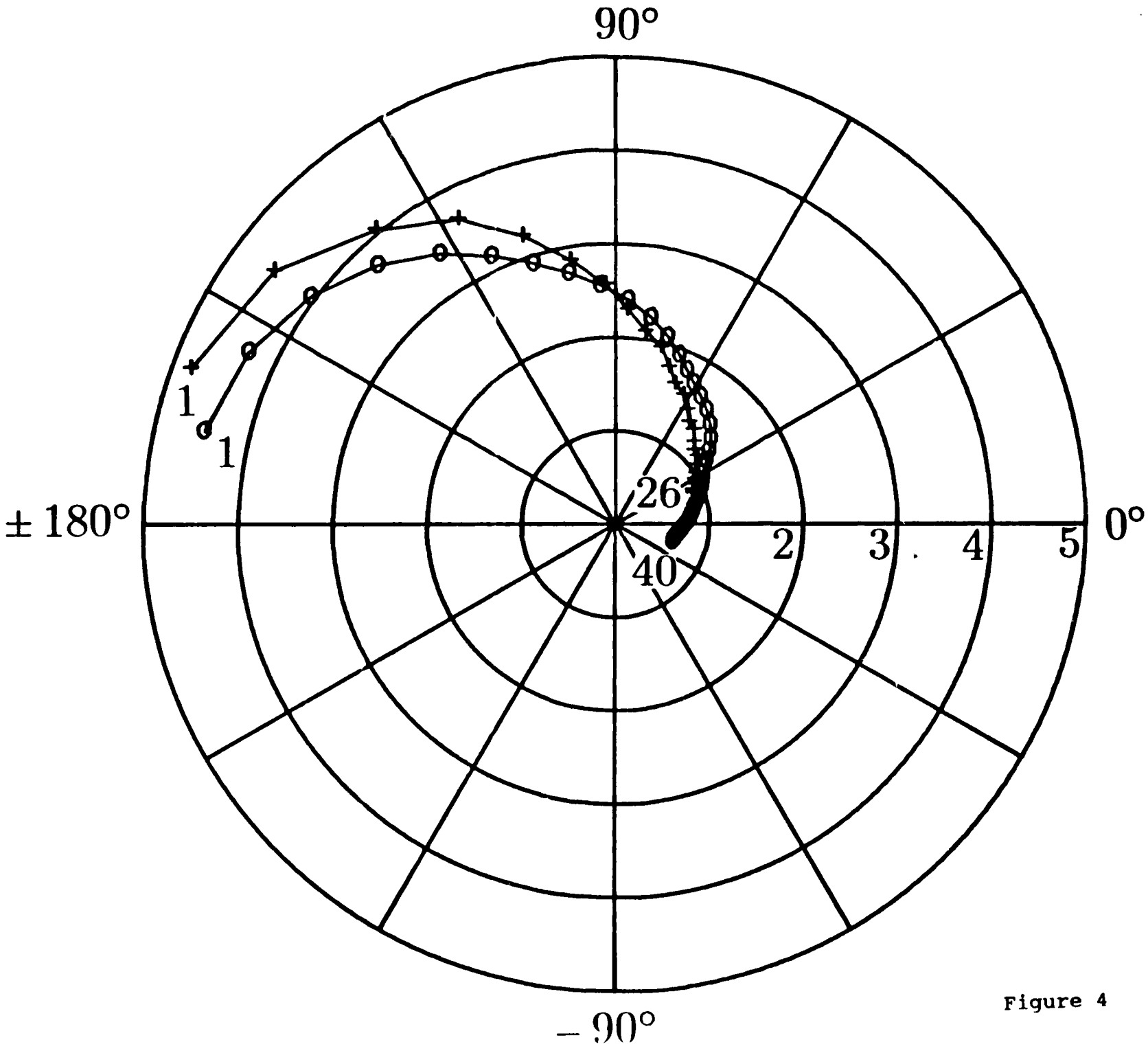

Figure 4

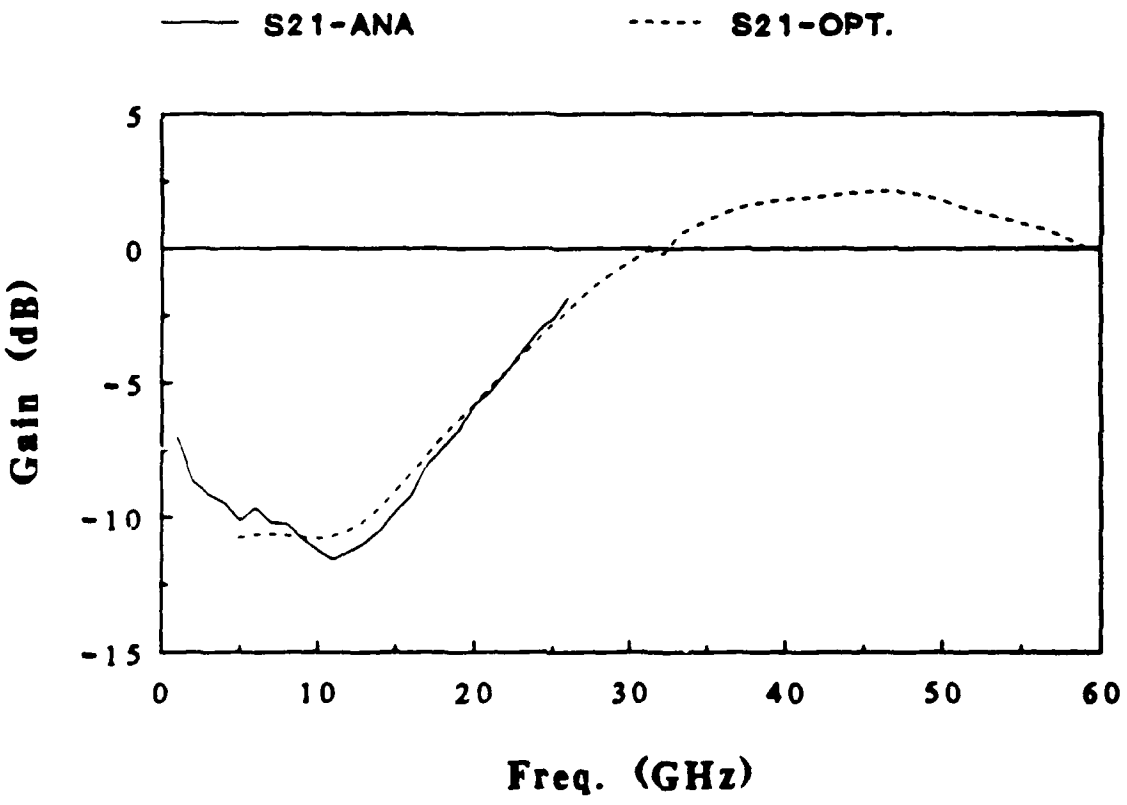

Figure 5 Comparison between optically measured magnitude of S_{21} (dashed line from 1-60 GHz) of the MMIC amplifier and network analyzer measurement (1-26 GHz).

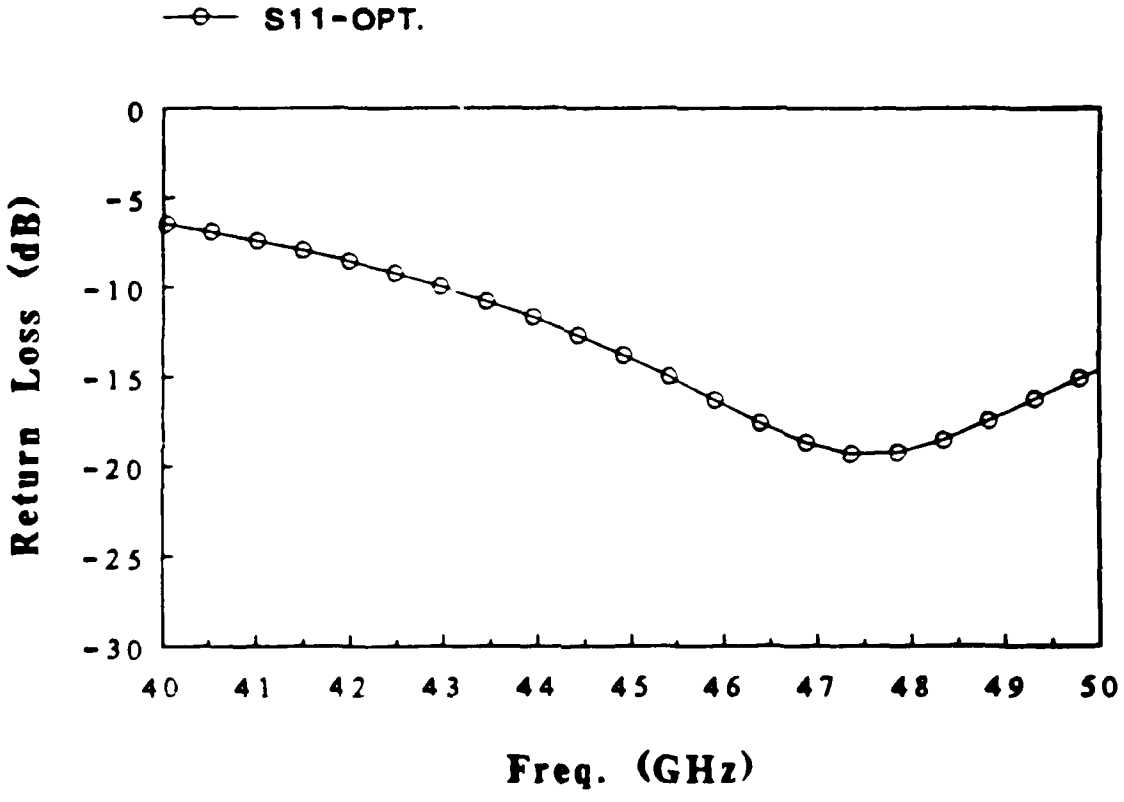

Figure 6a *Input return-loss versus frequency of the MMIC amplifier measured with the picosecond optoelectronic system.*

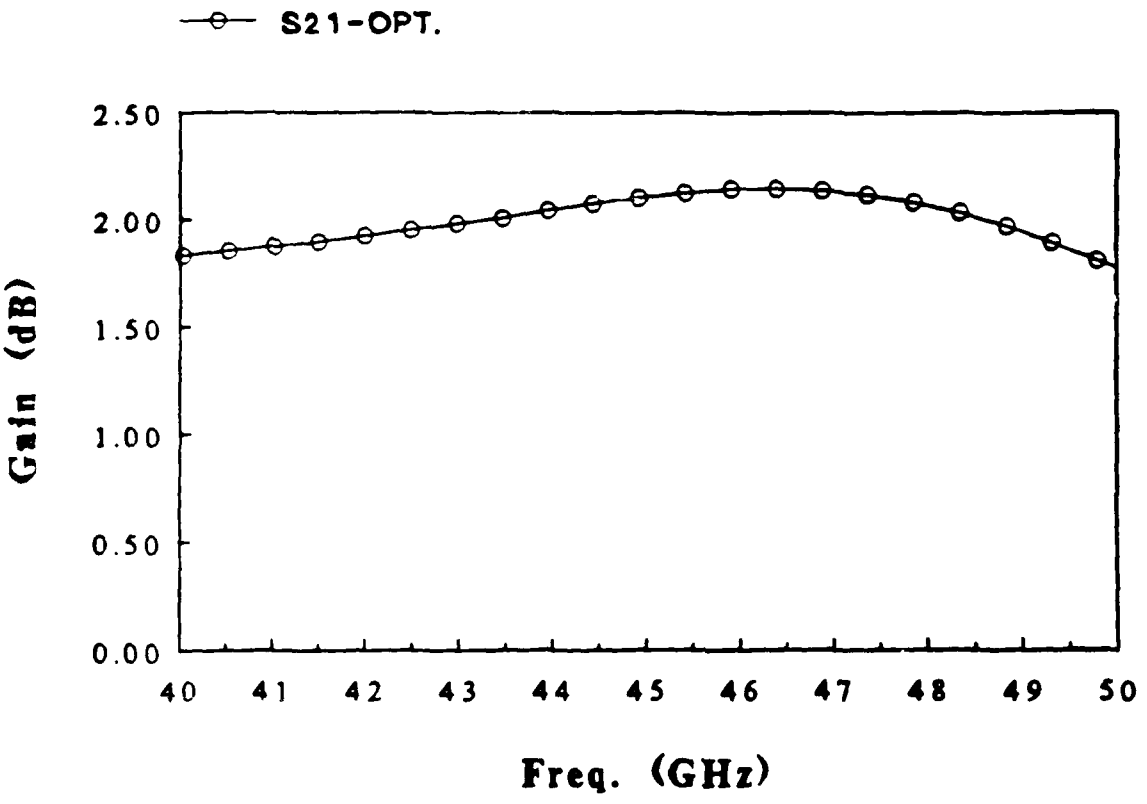

Figure 6b Gain versus frequency of the MMIC amplifier measured with the picosecond optoelectronic system.

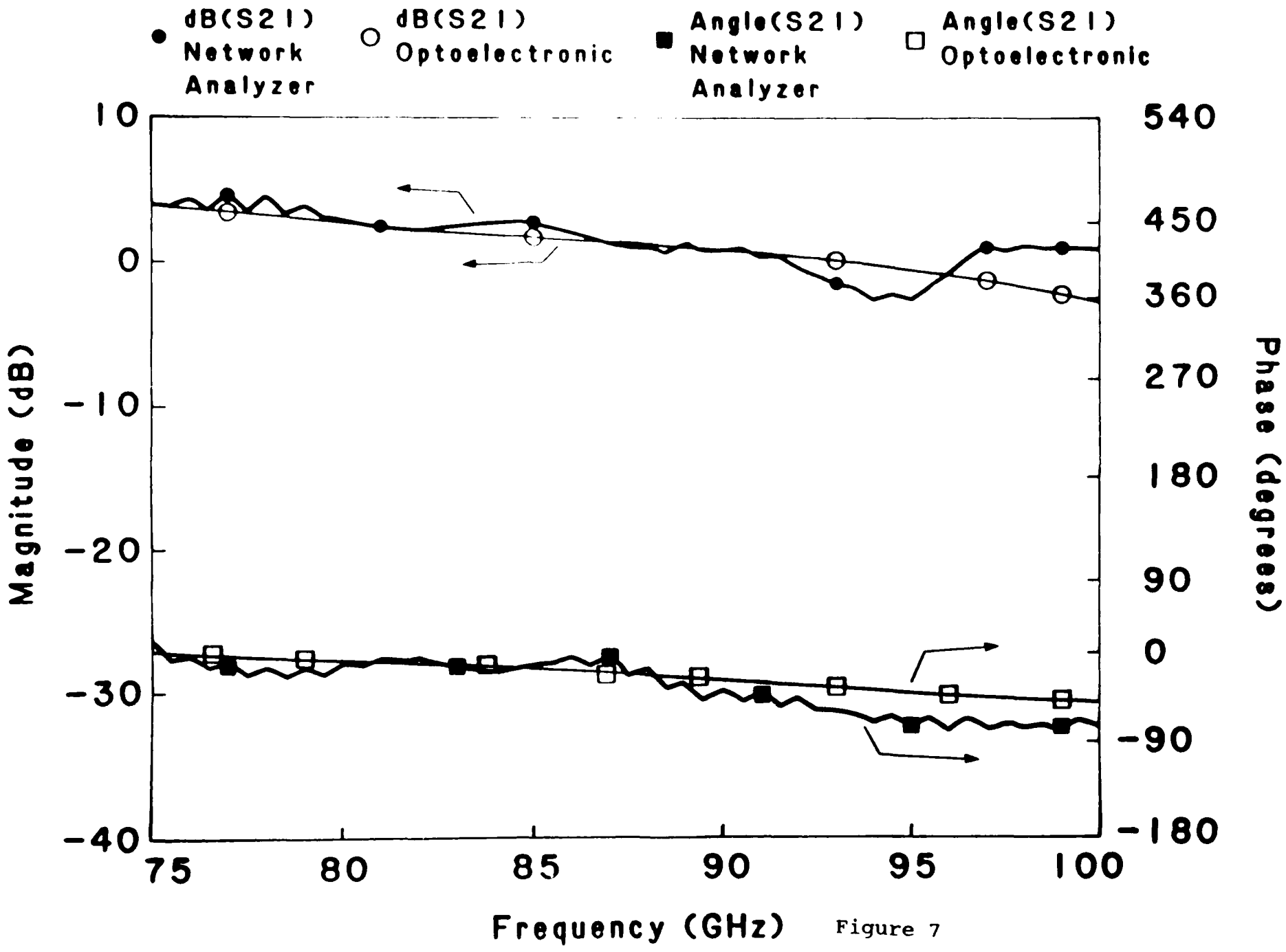
dB(S21) Network Analyzer
dB(S21) Optoelectronic
Angle(S21) Network Analyzer
Angle(S21) Optoelectronic
10
0
-10
-20
-30
-40
Magnitude (dB)
540
450
360
270
180
90
0
-90
-180
Phase (degrees)
75
80
85
90
95
100
Frequency (GHz)

Figure 7

GHz. is displayed in figure 9. By modulating the gate of the transistor we were able to generate a continous frequency coverage and plot out the transmission of a filter as shown in figure 10. The full paper is included as paper #3 in the appendix. A fourth paper on Superconductivity measurements is in preparation at this time.

CONCLUSION

The goals of the original program have been realized and now the instrumentation is being extended to infrared and shorter pulse measurements in a number of systems. Since the start of the program we have now moved up to measurements using subpicosecond switches and novel high frequency devices. This system turned out to be one of the most rewarding program in our effort. We are currently trying to expand and enhance its performance.

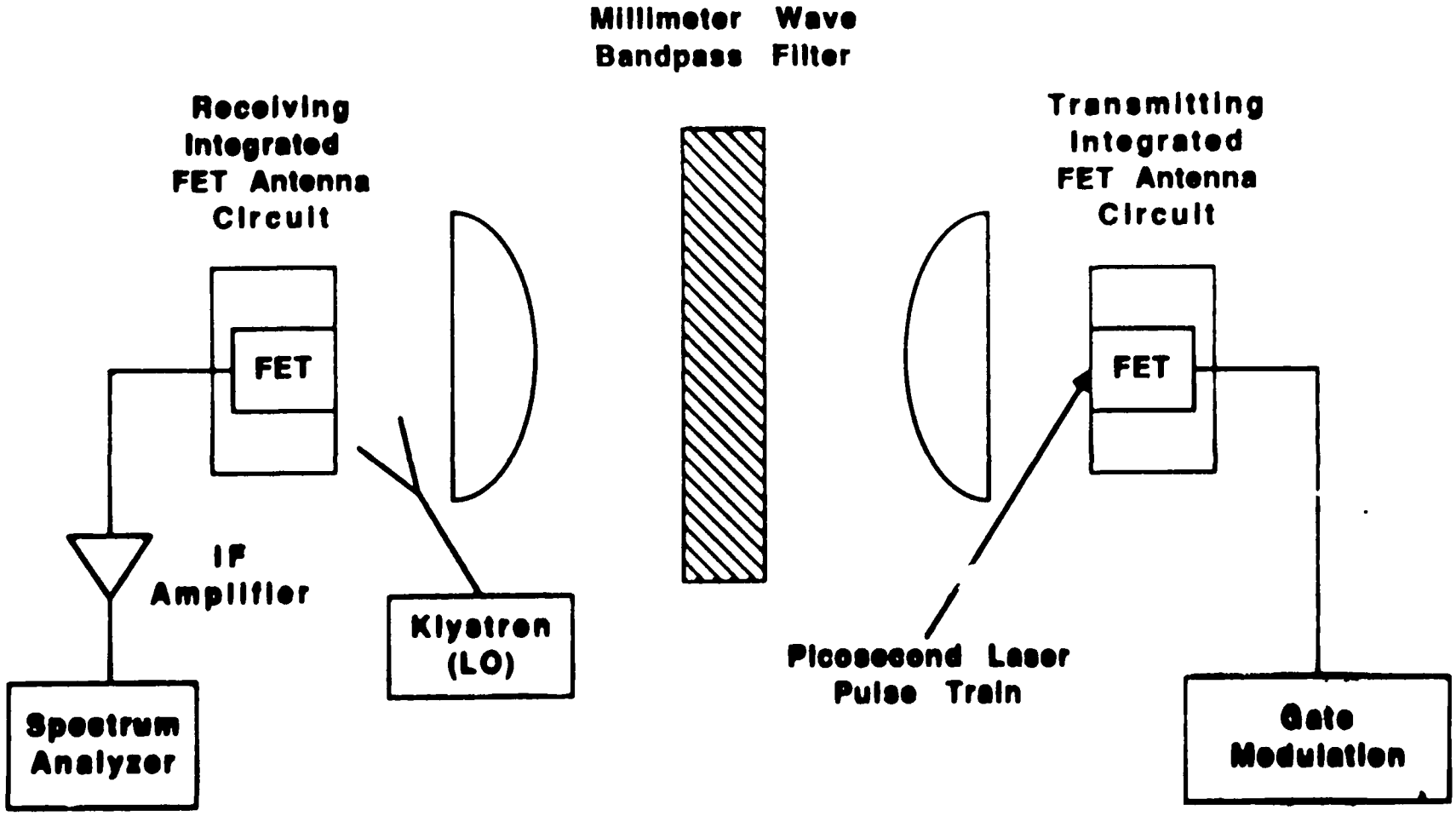
Millimeter Wave
Bandpass Filter
Receiving
Integrated
FET Antenna
Circuit
FET
IF
Amplifier
Klystron
(LO)
Spectrum
Analyzer
Transmitting
Integrated
FET Antenna
Circuit
FET
Picosecond Laser
Pulse Train
Gate
Modulation

Figure 8

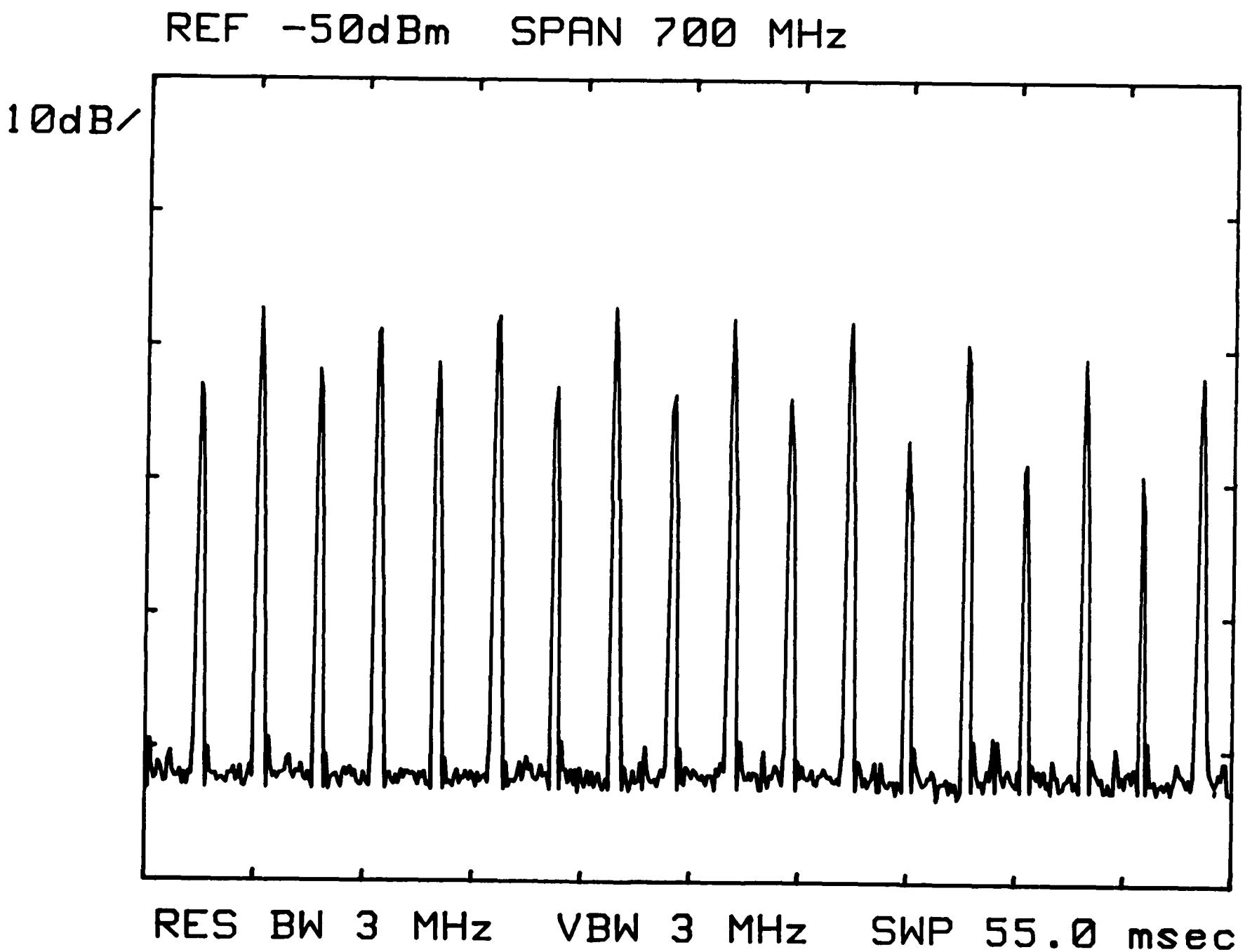

Figure 9

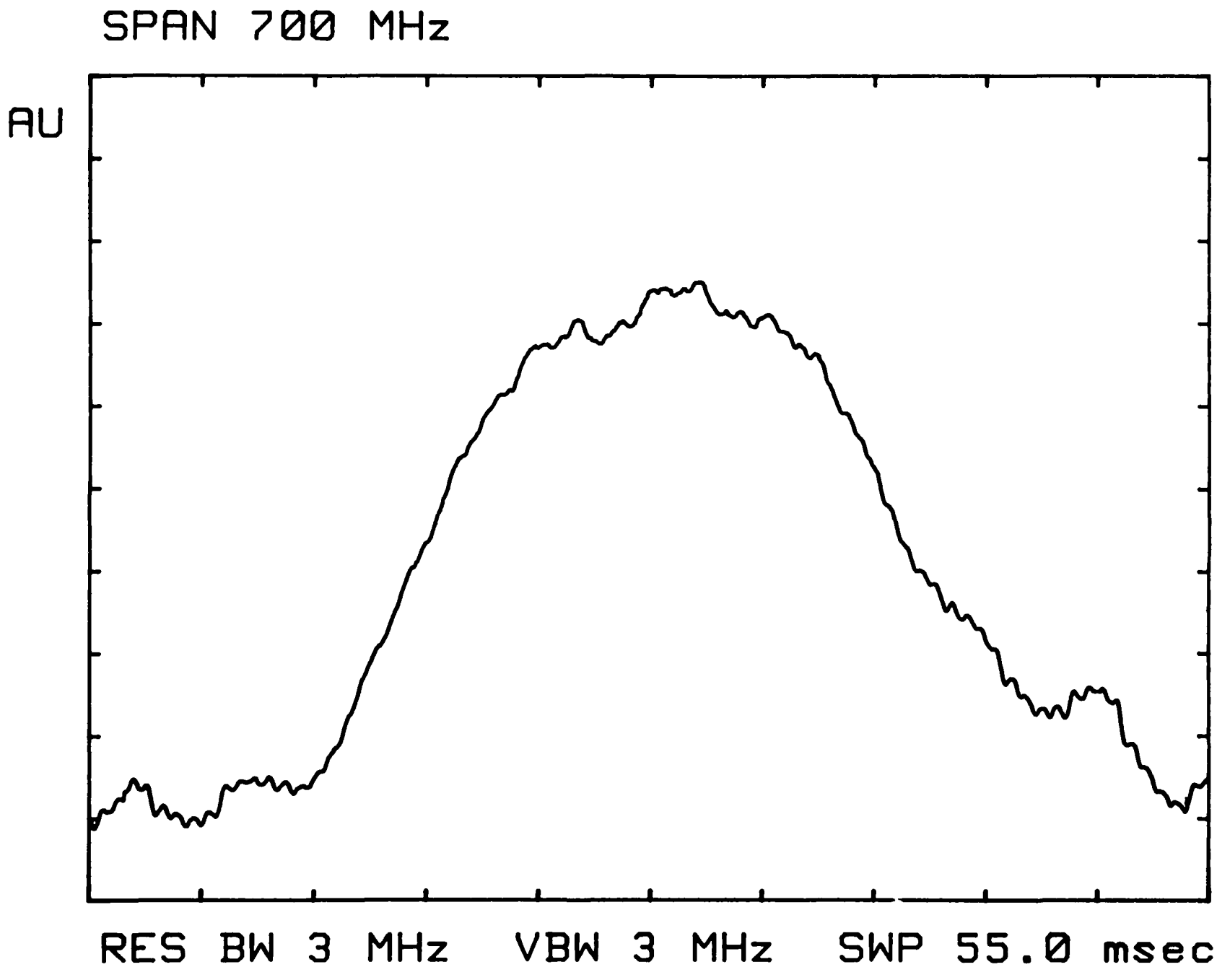

Figure 10

T-MTT/38/5//34524

Picosecond Optoelectronic Measurement of *S* Parameters and Optical Response of an AlGaAs/GaAs HBT

M. Matloubian
H. Fetterman
M. Kim
A. Oki
J. Camou
S. Moss
D. Smith

Reprinted from
IEEE TRANSACTIONS ON MICROWAVE THEORY AND TECHNIQUES
Vol. 38, No. 5, May 1990

Picosecond Optoelectronic Measurement of *S* Parameters and Optical Response of an AlGaAs/GaAs HBT

M. MATLOUBIAN, MEMBER, IEEE, H. FETTERMAN, FELLOW, IEEE, M. KIM, MEMBER, IEEE, A. OKI, MEMBER, IEEE, J. CAMOU, S. MOSS, MEMBER, IEEE, AND D. SMITH

Abstract—The *S* parameters of an AlGaAs/GaAs heterojunction bipolar transistor (HBT) were measured using a picosecond optoelectronic system. The measured *S* parameters show qualitatively good agreement with those obtained using a conventional vector network analyzer. The optical response of the HBT was also measured using this system by directly illuminating the base-collector region. Used as a phototransistor, the HBT showed pulse widths with FWHM as short as 15 ps.

I. Introduction

In recent years there has been steady progress in the development of high-frequency semiconductor devices and millimeter-wave integrated circuits. Present high-frequency transistors have cutoff frequencies well beyond the bandwidth that can be measured conveniently using conventional network analyzers. As a result, the millimeter-wave *S* parameters of devices are commonly calculated from the extrapolation of small-signal models of the transistor based on the microwave measurements. This extrapolation method has not been proven to be reliable in predicting the behavior of devices at frequencies much higher than the measured frequency. By using external mixers the present bandwidth of network analyzers has been extended to about 110 GHz. But several difficulties arise in characterizing devices in the millimeter-wave region. At high frequencies the transistors have to be mounted in test fixtures with waveguide-to-microstrip transitions. It is difficult to design wide-bandwidth and low-loss waveguide-to-microstrip transitions. The actual *S* parameters of the device have to be de-embedded from the test fixture, and with transitions having a high insertion loss erroneous results can be obtained.

Use of time-domain techniques for characterization of devices offers advantages over the frequency-domain techniques used by most network analyzers. By measuring the response of the device in the time domain and taking the Fourier transform of the data, the frequency performance of the device can be calculated. The response of the device can be "windowed" in the time domain and separated from reflections due to transitions and other unwanted signals before it is analyzed. This will simplify de-embedding of the *S* parameters of devices. But the use of time-domain techniques for device characterization has been very limited due to a lack of availability of fast electrical pulse generators and oscilloscopes.

In order to improve and optimize the performance of millimeter-wave transistors it is important to have a simple technique for direct characterization of devices at very high frequencies. Picosecond optoelectronic techniques offer a new method for generating and sampling ultrafast electrical pulses [1]–[3]. These electrical pulses can be used to test the response of high-speed semiconductor devices [4] and integrated circuits [5], [6]. Using photoconductive switches, picosecond electrical pulses can be generated and sampled at a very short distance from a device. Therefore, the high-frequency signals do not have to travel through long sections of transmission lines and waveguide transitions, making this technique superior to conventional network analyzers. In this study, *S* parameters and the optical response of AlGaAs/GaAs heterojunction bipolar transistors (HBT's), which are very promising devices for applications in microwave and millimeter-wave integrated circuits [7], were characterized using picosecond optoelectronic techniques.

II. Measurement

An AlGaAs/GaAs HBT was mounted in an optoelectronic test fixture of the type shown in Fig. 1. The HBT tested had $3 \times 10\ \mu m^2$ emitter and self-aligned base ohmic metal. The structure and fabrication of this device were previously reported in detail [8]. The microstrip lines were fabricated using gold on silicon-on-sapphire (SOS) substrates. A thin layer of chromium was used to improve adhesion between the gold and the silicon surface. The sapphire substrates were about 125 μm thick and the microstrip lines were designed to have a 50 Ω impedance. The silicon epi-layer was about 0.5 μm thick and was heavily implanted with four different energies of silicon ions to shorten the carrier lifetime to subpicosecond levels [9].

On each side of the device there are two photoconductive switches, which consist of 25 μm gaps in the side microstrip lines. By applying a dc bias to a photoconductive switch and focusing a

Manuscript received July 25, 1989; revised December 1, 1989. The UCLA portion of this work was supported by TRW under the California MIRO Program and by the Air Force Office of Scientific Research.

M. Matloubian and H. Fetterman are with the Department of Electrical Engineering, University of California, Los Angeles, Los Angeles, CA 90024.

M. Kim, A. Oki, and J. Camou are with the Electronic Systems Group, TRW, Redondo Beach, CA 90278.

S. Moss and D. Smith are with the Chemistry and Physics Laboratory, the Aerospace Corporation, Los Angeles, CA 90009.

IEEE Log Number 9034524

0018-9480/90/0500-0683$01.00 ©1990 IEEE

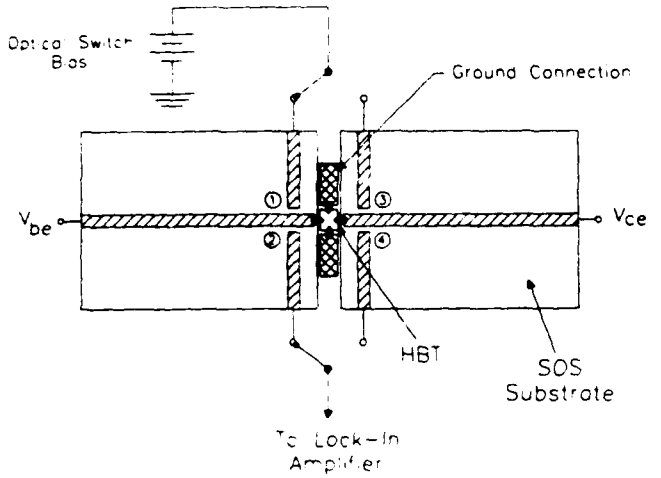

Fig. 1. Picosecond optoelectronic test fixture with an HBT wire-bonded to the center microstrip lines.

picosecond laser beam on the gap, fast electrical pulses are generated that propagate on the center transmission line. A second photoconductive switch is used for sampling the electrical pulses. The speed of the electrical pulse generated in our case is limited by the gap capacitance. The center microstrip lines, in addition to being used for launching the fast electrical pulses, are used to supply the dc biases to the transistor. This will allow the characterization of the device at any bias point. The center microstrip lines are made long enough that the reflections from the bias lines arrive at the sampling switch outside the "time window" necessary to measure the response of the device.

Fig. 2 shows the schematic of the picosecond optoelectronic system used to measure the S parameters of the HBT. The pump source for the dye laser is an actively mode-locked frequency-doubled Nd:YAG laser putting out 70 ps pulses at a wavelength of 532 nm and a repetition rate of 7.6 MHz. The dye laser uses rhodamine 6G (R6G) dye and has a cavity dumper which allows the repetition rate of the pulses to be varied. The dye laser is operated at a wavelength of 600 nm with a repetition rate of 3.8 MHz and an average power of 70 mW. The optical pulses have a pulse width of 1.2 ps measured using an optical autocorrelator. The train of picosecond laser pulses from the dye laser is split into two beams. The first beam passes through an optical chopper and is focused onto one of the pulse-generating switches on the optoelectronic test fixture. The second beam travels a path with a variable length and is focused onto one of the sampling switches. The length of this path can be varied very precisely by moving a computer-controlled translation stage. The path length of the second beam can be varied in such a way that it arrives at the sampling switch before, during, or after the arrival of the optical pulse at the generation switch. The output from the sampling switch is fed into the input of the lock-in amplifier. Depending on which of the four optical switches is used as the generator and which is used as the sampler, the HBT can be characterized completely in the time domain. By taking the Fourier transform of the reflected and transmitted signals and normalizing it to the Fourier transform of the appropriate input signal, the S parameters of the device can be determined [4].

III. Results

Fig. 3(a) shows the input reflection of the HBT measured by using switch 1 as the pulse generator and sampling switch 2. The first peak in the figure corresponds to the electrical autocorrelation of the input pulse to the device. As the delay of the sampling pulse was varied the reflection from the bond wires and then the reflection from the device were obtained. To analyze the data, the autocorrelation signal was separated from the bond wires and device reflections. Then the reflection of the bond wires was also "windowed out." Since a 1.5 mm section of microstrip transmission line separates the device from the sampling point, the reference plane of the measurement has to be moved to account for the phase change. This can be done very simply in the time domain by time shifting the reflected signal. Dispersion of electrical pulses over this length of microstrip line was neglected [10]. By taking the ratio of the Fourier transform of the reflected signal to the autocorrelation signal, the input reflection coefficient (S_{11}) of the HBT can be determined.

To measure the input gain of the transistor (S_{21}), switch 1 was used as the pulse generator and switch 4 as the sampler. The result shown in Fig. 3(b) shows the electrical pulse that has been broadened to about 35 ps by passing through the transistor. Again, this pulse has to be time-shifted to account for the short length of the microstrips on both sides of the device. S_{21} of the HBT can be determined by taking the Fourier transform of this pulse and normalizing it to the effective input signal from the optical switches after a calibration procedure. Similarly, the reverse transmission and output reflection of the HBT were also measured and then S_{12} and S_{22} were determined from these measurements.

The optically measured S_{21} of the HBT is shown in Fig. 4 for the frequency range of 1–40 GHz. For comparison S parameters of a similar HBT were measured using on-wafer RF probes and a conventional vector network analyzer (HP8510). The network analyzer measured S_{21} for the range of 1–26 GHz is also shown in Fig. 4. From the measured S parameters, the maximum available gain (MAG) of the device was calculated. The plot of MAG versus frequency (maximum stable gain (MSG) for conditionally stable case) for both the optoelectronic measurements and the network analyzer measurements is shown in Fig. 5. Except for some discrepancies, the two measurement techniques are in good agreement. The discrepancies are believed to be due to the effect of the bond wires on the optically measured S parameters and to slight differences between the two HBT's tested.

IV. Optical Response

HBT's are also important in applications such as high-speed optical detectors for optical communication [11] and for optical control of MMIC's [12]. As a result, it is important to measure the speed of the HBT as a photodetector. Using picosecond optoelectronic techniques the speed of photodetectors can be measured [13]. The same optoelectronic test fixture used in the S parameter measurements was used to measure the speed of the HBT as an optical detector. In this case the optical generation pulse was focused onto the HBT and the output signal was sampled at switch 4. In these measurements the base of the HBT was floating and the device was tested as a phototransistor. Since this device has a self-aligned base metal, the separation between the base fingers and the emitter edge is only about 0.15 μm [8]. As a result the laser pulse penetrates the device only between the base and the collector fingers. For a wavelength of 600 nm the penetration depth in GaAs is about 2000 Å [14]. With base and collector thicknesses of 1500 Å and 5000 Å, respectively, more than 95% of the light absorption will occur within these two layers.

The optical response of the HBT for a collector-to-emitter voltage of 3 V is shown in Fig. 6. The pulse has a FWHM of about 15 ps, which is very fast considering the device does not

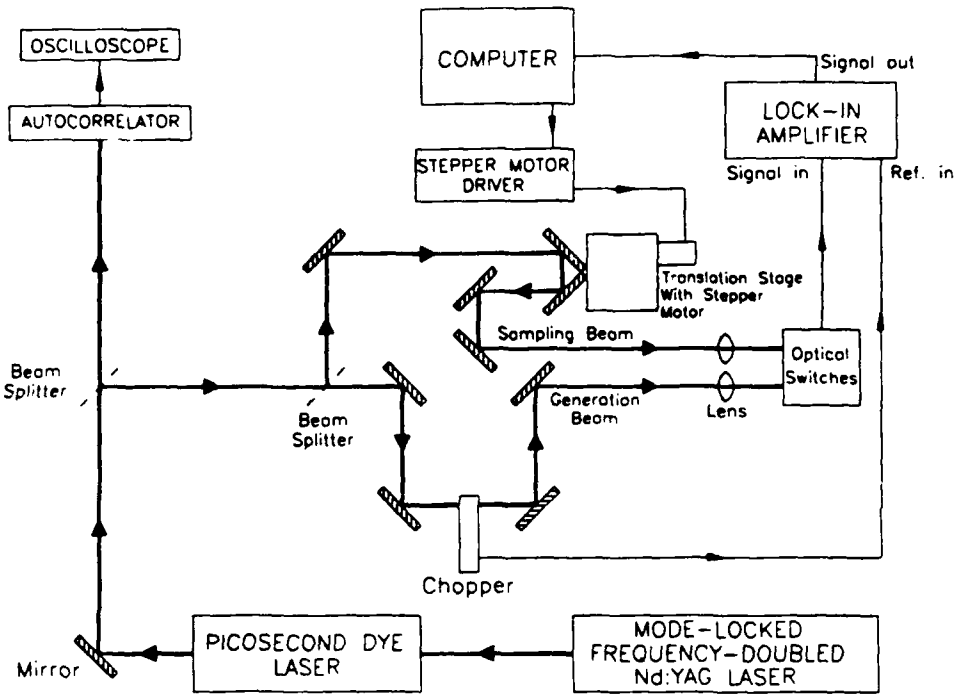

Fig. 2. Experimental setup for generation and sampling of fast electrical pulses using a computer-controlled optical time delay.

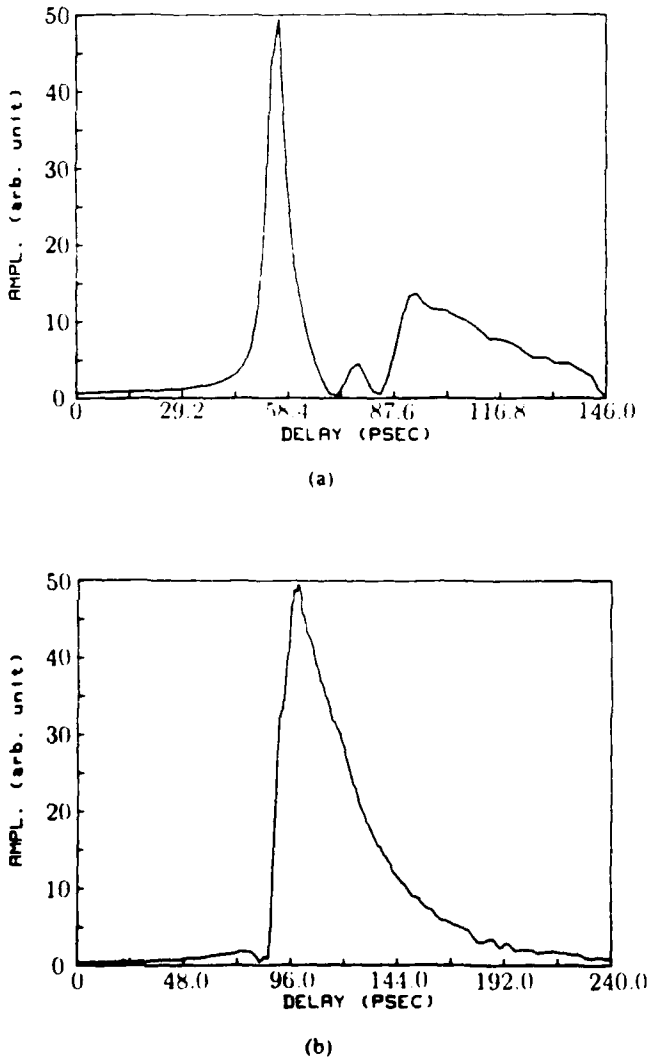

Fig. 3. (a) Input reflection measurement of the HBT using switch 1 as the pulse generator and sampling switch 2. (b) Forward transmission measurement using switch 1 as the pulse generator and sampling switch 4.

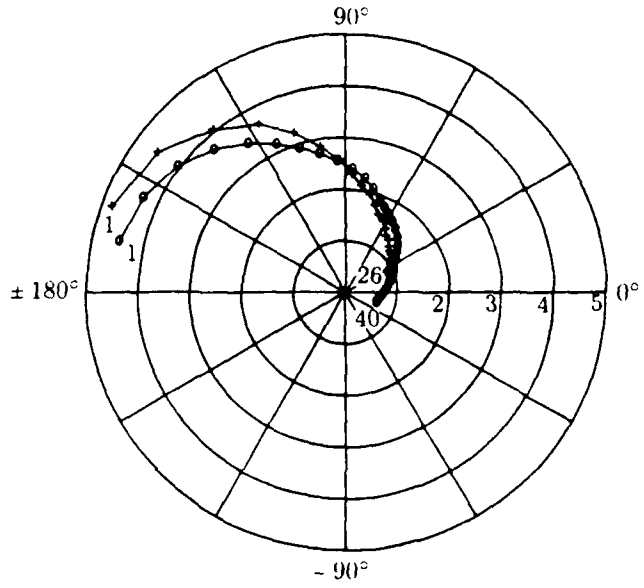

Fig. 4. Comparison between optically measured S_{21} of the HBT (∘) from 1 to 40 GHz and network analyzer measurement (+) from 1 to 26 GHz.

have a built-in field in the base region. The pulse width of the optical response of the HBT versus the collector-to-emitter voltage is shown in Fig. 7. As can be seen from this figure, the pulse width decreases from about 55 ps at 0 V to 15 ps at 3 V and remains constant for higher voltages. Comparing Fig. 6 with Fig. 3(b), it is observed that a much faster response time was obtained by directly injecting an optical signal into the HBT (bypassing the base input). This demonstrates that this device is intrinsically fast and that the electrical performance is limited by the base resistance.

V. Conclusion

S parameters of an HBT were measured up to 40 GHz using a picosecond optoelectronic technique. The results show qualitatively good agreement with measurements of a similar HBT using

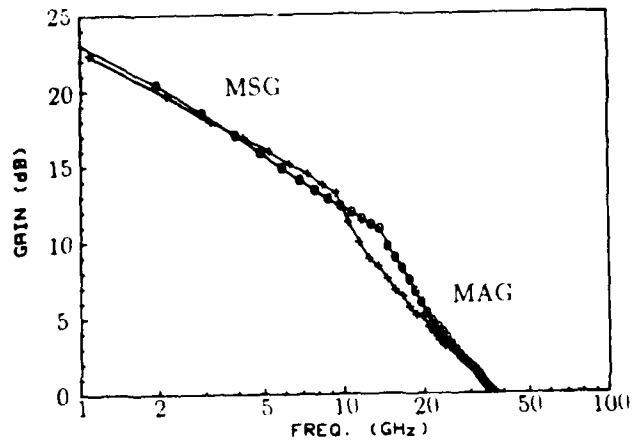

Fig. 5. Maximum available gain (MAG), maximum stable gain (MSG) versus frequency of the AlGaAs/GaAs HBT calculated from the measured S parameters by the optoelectronic system (+) and from network analyzer measurement (-).

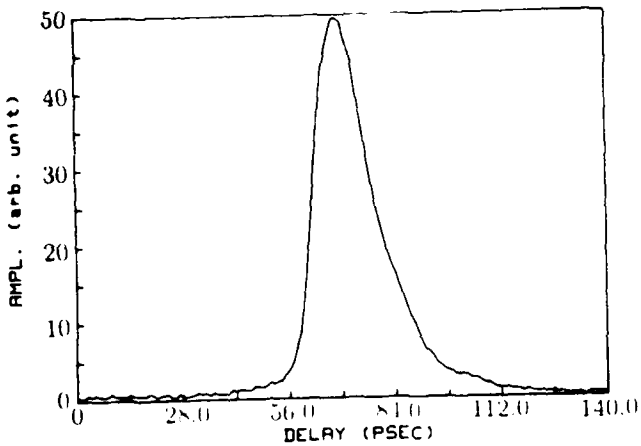

Fig. 6. Optical response of the HBT used as a phototransistor for $V_{ce} = 3$ V.

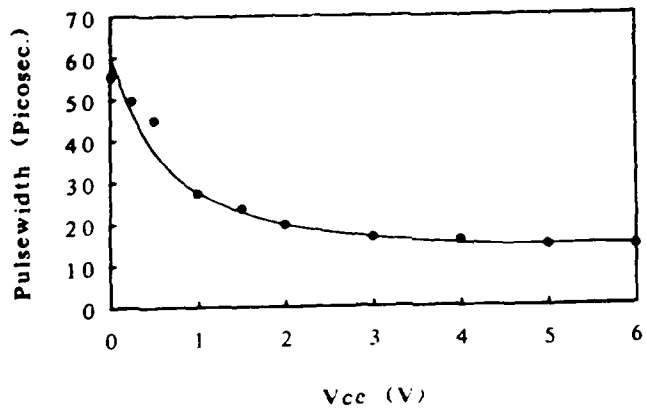

Fig. 7. Variation of the optical response pulse width as a function of the collector-to-emitter voltage.

on-wafer RF probes and a conventional vector network analyzer over the bandwidth of the network analyzer (26 GHz). The optoelectronically measured S parameters of the device were limited by the cutoff frequency of the device. The system itself has a bandwidth greater than 150 GHz. New HBT's with higher cutoff frequencies are currently being characterized. The optical response of the HBT was also measured using this system. HBT's appear to be very promising as high-speed optical detectors. Although in this study the optical switches were fabricated on a different substrate than the device, it is possible to integrate optical switches with devices on the same wafer and remove the effect of the bond wires on the measurements. This will allow on-wafer measurement of S parameters over a wide bandwidth.

REFERENCES

[1] D. H. Auston, "Impulse response of photoconductors in transmission lines," *IEEE J. Quantum Electron.*, vol. QE-19, no. 4, pp. 639–648, 1983.
[2] K. J. Weingarten, M. J. W. Rodwell, and D. M. Bloom, "Picosecond optical sampling of GaAs integrated circuits," *IEEE J. Quantum Electron.*, vol. QE-24, no. 2, pp. 198–220, 1988.
[3] J. A. Valdmanis and G. Mourou, "Subpicosecond electrooptic sampling: Principles and applications," *IEEE J. Quantum Electron.*, vol. QE-22, no. 1, pp. 69–78, 1986.
[4] D. E. Cooper and S. C. Moss, "Picosecond optoelectronic measurement of the high-frequency scattering parameters of a GaAs FET," *IEEE J. Quantum Electron.*, vol. QE-22, no. 1, pp. 94–100, 1986.
[5] P. Polak-Dingles *et al.*, "On wafer characterization of monolithic millimeter-wave integrated circuits by picosecond optical electronic technique," in *IEEE MTT-S Int. Microwave Symp. Dig.*, 1988, pp. 237–240.
[6] R. K. Jain, D. E. Snyder, and K. Stenersen, "A new technique for the measurement of speeds of gigahertz digital IC's," *IEEE Electron Device Lett.*, vol. EDL-5, no. 9, pp. 371–373, 1984.
[7] P. M. Asbeck *et al.*, "Heterojunction bipolar transistors for microwave and millimeter-wave integrated circuits," *IEEE Trans. Microwave Theory Tech.*, vol. MTT-35, no. 12, pp. 1462–1470, 1987.
[8] A. K. Oki, M. E. Kim, G. M. Gorman, and J. B. Camou, "High-performance GaAs heterojunction bipolar transistor logarithmic IF amplifier," *IEEE Trans. Microwave Theory Tech.*, vol. 36, no. 12, pp. 1958–1965, 1988.
[9] S. C. Moss, J. F. Knudsen, and D. D. Smith, "Linearity of response of ultrafast photoconductive switches: critical dependence upon ion-implantation and fabrication condition," *J. Modern Opt.*, vol. 35, no. 12, pp. 2007–2030, 1988.
[10] D. E. Cooper, "Picosecond optoelectronic measurement of microstrip dispersion," *Appl. Phys. Lett.*, vol. 47, no. 1, pp. 33–35, 1985.
[11] F. Capasso, W. T. Tsang, C. G. Bethea, A. L. Hutchinson, and B. F. Levine, "New graded band-gap picosecond phototransistor," *Appl. Phys. Lett.*, vol. 42, no. 1, pp. 93–95, 1983.
[12] R. N. Simons, "Microwave performance of an optically controlled AlGaAs/GaAs high electron mobility transistor and GaAs MESFET," *IEEE Trans. Microwave Theory Tech.*, vol. MTT-35, no. 12, pp. 1444–1455, 1987.
[13] D. H. Auston and P. R. Smith, "Picosecond optical electronic sampling: Characterization of high-speed photodetectors," *Appl. Phys. Lett.*, vol. 41, no. 7, pp. 599–601, 1982.
[14] E. D. Palik, *Handbook of Optical Constants of Solids*. New York: Academic Press, 1985.

Wide Band Millimeter Wave Characterization of Sub-0.2 Micrometer Gate-Length AlInAs/GaInAs HEMTs

Mehran Matloubian*, Member, IEEE, Steven E. Rosenbaum*, Member, IEEE, Harold R. Fetterman*, Fellow, IEEE, and Paul T. Greiling†, Fellow, IEEE

* Department of Electrical Engineering, University of California, Los Angeles, CA 90024
† Hughes Aircraft Company, Research Laboratories, Malibu, CA 90265

Abstract

The S parameters of an AlInAs/GaInAs high electron mobility transistor (HEMT) were measured using a picosecond optoelectronic system over a bandwidth of 100 GHz. These picosecond optoelectronic measurements were validated by comparing low frequency measurements to those obtained using on wafer RF probes/vector network analyzer, and W-band results to measurements done using a waveguide-to-microstrip transition/vector network analyzer frequency extender. This is the widest bandwidth of measured S parameters reported on a single transistor.

I. INTRODUCTION

High electron mobility transistors (HEMTs) are increasingly replacing GaAs MESFETs in microwave and millimeter wave circuits [1,2]. Their higher cutoff frequencies combined with lower noise make them more attractive in applications such as millimeter wave low noise amplifiers [3] and mixers [4]. In particular $Al_{0.48}In_{0.52}As/Ga_{0.47}In_{0.53}As$ HEMTs have demonstrated superior performance over HEMTs made from other material systems [5,6]. However, these transistors have cutoff frequencies well beyond the bandwidth that can be measured conveniently using conventional network analyzers. As a result only a small amount of data exists describing the performance of HEMTs in the W-band. By using external mixers the present bandwidth of network analyzers has been extended to about 100 GHz. But several difficulties arise in characterization of devices in the millimeter wave region. At high frequencies the transistors have to be mounted in test fixtures with waveguide-to-microstrip transitions. It is difficult to design wide bandwidth waveguide-to-microstrip transitions that have low insertion and return loss. The actual S parameters of the transistor have to be de-embedded from the test fixture and using transitions having a high insertion/return loss can cause erroneous results.

In order to improve and optimize performance of millimeter wave transistors it is important to have a simple technique for direct characterization of devices at very high frequencies. Using picosecond optoelectronic techniques ultrafast electrical pulses can be generated and sampled [7,8,9]. These electrical pulses can be used to test the response of high speed semiconductor devices [10] and integrated circuits [11] over a wide bandwidth. Using photoconductive switches, picosecond electrical pulses can be generated and sampled at a very short distance from a device. Therefore, the high frequency signals do not have to travel through long sections of transmission lines and waveguide transitions, making this technique superior to conventional network analyzers. In this study S parameters of $Al_{0.48}In_{0.52}As/Ga_{0.47}In_{0.53}As$ HEMTs were measured using picosecond optoelectronic tech-

niques over a 100 GHz bandwidth. To validate the optoelectronic measurements the S parameters were also measured using on wafer RF probes/network analyzer (over the frequency range of 1-26 GHz) and a network analyzer frequency extender (over the frequency range of 75-100 GHz).

II. Measurements

The cross section of the $Al_{0.48}In_{0.52}As/Ga_{0.47}In_{0.53}As$ HEMT is shown in figure 1. The gate-length of the transistor is less than 0.2 μm with a gate-width of 50 μm. The maximum transconductance of the device is greater than 1000 ms/mm. For the optoelectronic measurements the AlInAs/GaInAs HEMT was mounted in a test fixture as shown in figure 2. The microstrip lines were fabricated using Cr/Au on silicon-on-sapphire (SOS) substrates. The sapphire substrates were about 125 μm thick and the microstrip lines were designed to have a 50 Ω impedance. The silicon epi-layer was about 0.5 μm thick and was heavily implanted with silicon ions to shorten the carrier lifetime.

On each side of the HEMT there are two photoconductive switches which consist of 25 μm gaps in the side microstrip lines. By applying a DC bias to a photoconductive switch and focusing a picosecond laser beam on the gap, fast electrical pulses are generated that propagate on the center transmission line. A second photoconductive switch is used for sampling of the electrical pulses. The details of the measurements are described elsewhere [12].

Depending on which one of the four optical switches is used as the generator and which one as the sampler the HEMT can be characterized completely in the time-domain. By taking the Fourier transform of the reflected and transmitted signals and normalizing it to the Fourier transform of the appropriate input signal the S parameters of the device can be determined [10].

III. Results

Using the picosecond optoelectronic system the time-domain response of the HEMT was measured and the S parameters of the HEMT were determined over a bandwidth of 100 GHz. This is the widest bandwidth of S parameters measured on a single transistor. To validate these measurements the S parameters of similar HEMTs were measured using on wafer RF probes and a conventional network analyzer (HP8510) over the frequency of 1-26 GHz. From the measured S parameters the maximum available gain (MAG) of the device was calculated. The plot of MAG versus frequency (maximum stable gain (MSG) for conditionally stable case) for both the optoelectronic measurements and network analyzer measurements are shown in figure 3. Very good agreement can be seen between both techniques over the range of frequency overlap.

It is also important to find the accuracy of the optoelectronic measurements at millimeter wave frequencies. For this purpose an AlInAs/GaInAs HEMT was tested using a W-band (75-100 GHz) network analyzer frequency extender. The device was mounted in a W-band ridged waveguide-to-microstrip transition which consists of a Chebyshev stepped impedance transformer between the WR-10 waveguide and the 50 Ω microstrip transmission line [13]. This type of transition was chosen for it's broad-band characteristics with a center frequency of 90 GHz and a passband from 70 to 110 GHz. The microstrip transmission lines were fabricated on 0.005 in. fused silica. The return loss of the fixture was measured to be more than 5 dB and the insertion was less than 5 dB across the band. The measured data was de-embedded from the fixture response using a two tiered technique [13].

Figures 4(a)-4(d) show comparison between S parameters measured by the optoelectronic system and network analyzer frequency extender over the range of 75-100 GHz. Measurement of the W-band test fixture revealed a distinct resonant waveguide mode propagating from input to output in addition to the microstrip transmission line. This resonance has a tendency to mask the performance of the device under test to some degree. Measurements of

S_{11} and S_{22} are affected most by the resonance; S_{21} and S_{12} are impacted to a lesser degree. The effect of this resonance on the transistor data may be seen as a distinct ripple in the magnitudes of all four S parameters and in the case of S_{22}, a complete masking of the phase. From figures 4(b) and 4(c) the agreement between S_{21} and S_{12} measurements using the two techniques is quite good. Due to the ripples in network analyzer measurements S_{11} and S_{22} results have discrepancies. Both the network analyzer and the picosecond optoelectronic measurements show the effects of source inductance due to the bond wires. This will be discussed in connection with the equivalent circuit model and high frequency performance elsewhere [14].

IV. Conclusion

S parameters of an AlInAs/GaInAs HEMT were measured using picosecond optoelectronic techniques over a bandwidth of 100 GHz. The results show good qualitative agreement with measurements of a similar HEMT using on-wafer RF probes and a conventional vector network analyzer over the bandwidth of the network analyzer (26 GHz). Comparison with measurements by a W-band network analyzer showed excellent agreement for S_{21} and S_{12} but there were limited by de-embedding in the case of S_{11} and S_{22}. This study demonstrates the advantages of wide bandwidth characterization of high frequency transistors using picosecond optoelectronic techniques.

Acknowledgments

The authors would like to thank Drs. U. Mishra, A. Brown, and M. Delaney for providing the HEMTs used in this study and Dr. J. East and B. Denheyer for help with the W-band measurements. This work was supported in part by the Hughes Research Labs. under the California MICRO program and in part by the Air Force Office of Scientific Research.

References

[1] P. M. Smith, P. C. Chao, K. H. G. Duh, L. F. Lester, B. R. Lee, and J. M. Ballingall, "Advances in HEMT Technology and Applications," *IEEE MTT-S Int. Microwave Symp. Digest*, pp. 749–752, 1987.

[2] U. K. Mishra, J. F. Jensen, A. S. Brown, M. A. Thompson, L. M. Jelloian, and R. S. Beaubien, "Ultra-High-Speed Digital Circuit Performance in 0.2-μm Gate-Length AlInAs/GaInAs HEMT Technology," *IEEE Electron Device Lett.*, vol. EDL-9, no. 9, pp. 482–484, 1988.

[3] S. Vaughn, K. White, U. K. Mishra, M. J. Delaney, P. Greiling, and S. Rosenbaum, "High Performance V-Band Low Noise Amplifiers," *IEEE MTT-S Int. Microwave Symp. Digest*, pp. 801–804, 1989.

[4] S. A. Maas, "Design and Performance of a 45-GHz HEMT Mixer," *IEEE Trans. Microwave Theory Tech.*, vol. MTT-34, no. 7, pp. 799–803, 1986.

[5] U. K. Mishra, A. S. Brown, S. E. Rosenbaum, C. E. Hooper, M. W. Pierce, M. J. Delaney, S. Vaughn, and K. White, "Microwave Performance of AlInAs-GaInAs HEMT's with 0.2- and 0.1- μm Gate Length," *IEEE Electron Device Lett.*, vol. EDL-9, no. 12, pp. 647–649, 1988.

[6] U. K. Mishra, A. S. Brown, M. J. Delaney, P. T. Greiling, and C. F. Krumm, "The AlInAs-GaInAs HEMT for Microwave and Millimeter-Wave Applications," *IEEE Trans. Microwave Theory Tech.*, vol. MTT-37, no. 9, pp. 1279–1285, 1989.

[7] D. H. Auston, "Impulse Response of Photoconductors in Transmission Lines," *IEEE J. Quantum Electron.*, vol. QE-19, no. 4, pp. 639–648, 1983.

[8] K. J. Weingarten, M. J. W. Rodwell, and D. M. Bloom, "Picosecond Optical Sampling of GaAs Integrated Circuits," *IEEE J. Quantum Electron.*, vol. QE-24, no. 2, pp. 198–220, 1988.

[9] J. A. Valdmanis and G. Mourou, "Subpicosecond Electrooptic Sampling: Principles and Applications," *IEEE J. Quantum Electron.*, vol. QE-22, no. 1, pp. 69–78, 1986.

[10] D. E. Cooper and S. C. Moss, "Picosecond Optoelectronic Measurement of the High-Frequency Scattering Parameters of a GaAs FET," *IEEE J. Quantum Electron.*, vol. QE-22, no. 1, pp. 94–100, 1986.

[11] P. Polak-Dingles, H-L. Hung, T. Smith, H. Huang, K. Webb, and C. H. Lee, "On Wafer Characterization of Monolithic Millimeter-Wave Integrated Circuits by Picosecond Optical Electronic Technique," *IEEE MTT-S Int. Microwave Symp. Digest*, pp. 237–240, 1988.

[12] M. Matloubian, H. Fetterman, M. Kim, A. Oki, J. Camou, S. Moss, and D. Smith, "Picosecond Optoelectronic Measurement of S Parameters and Optical Response of an AlGaAs/GaAs HBT," *IEEE Trans. Microwave Theory Tech.*, vol. MTT-38, no. 5, 1990.

[13] K. J. Moeller, J. H. Schaffner, and H. R. Fetterman, "W-band six-port network analyzer for two-port characterization of millimeter wave transistors," *Rev. Sci. Instrum.*, vol. 60, no. 3, pp. 433–438, 1989.

[14] M. Matloubian, S. E. Rosenbaum, H. R. Fetterman, and P. T. Greiling, "Modeling of AlInAs/GaInAs HEMTs at Microwave and Millimeter Wave Frequencies,". to be published.

List of Figures

Fig. (1) Cross section of the $Al_{0.48}In_{0.52}As/Ga_{0.47}In_{0.53}As$ HEMT.

Fig. (2) Picosecond optoelectronic test fixture with the HEMT wire-bonded to the center microstrip lines.

Fig. (3) Maximum available gain (MAG) / maximum stable gain (MSG) versus frequency of the AlInAs/GaInAs HEMT calculated from the measured S parameters by the optoelectronic system (O), and from network analyzer measurements using on wafer RF probes (•).

Fig. (4) Magnitude and phase versus frequency over the frequency range of 75-100 GHz for optically measured S parameters and measurements by network analyzer frequency extender (a) S_{11} (b) S_{21} (c) S_{12} (d) S_{22}

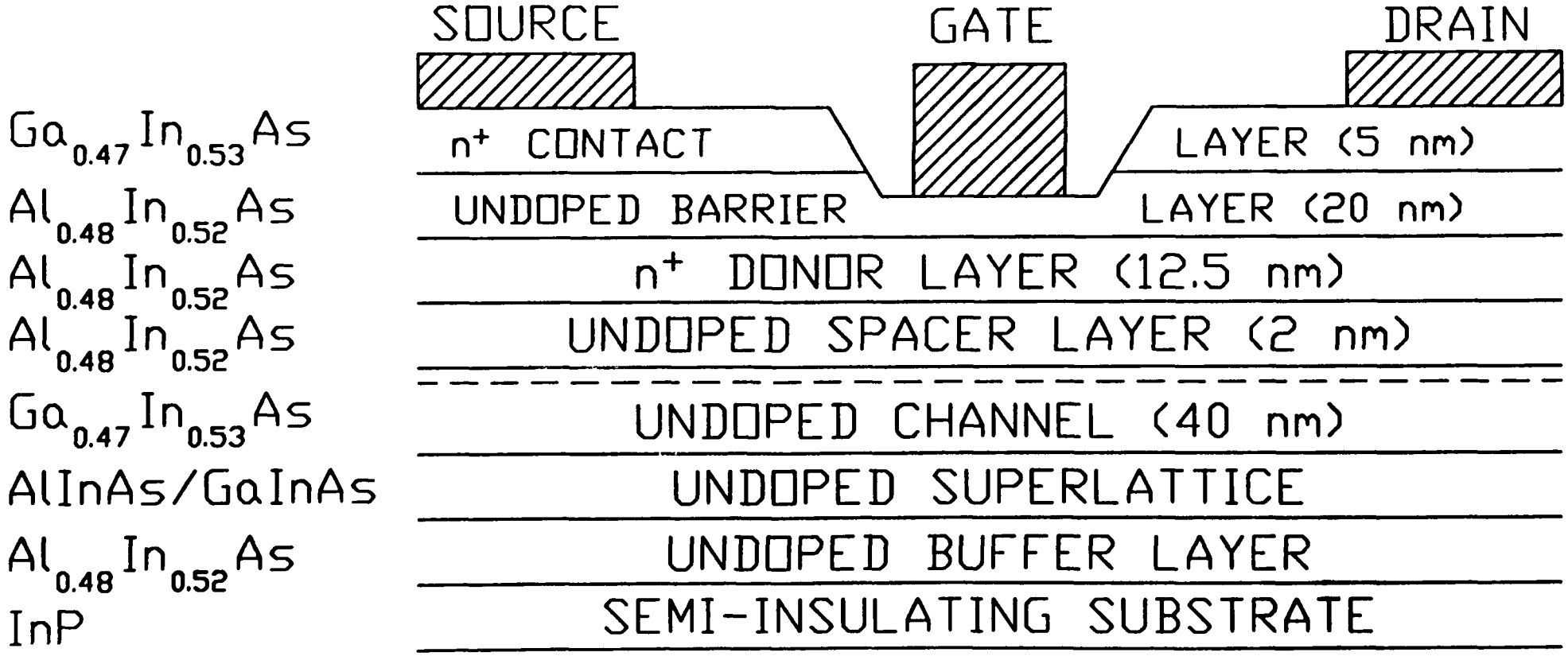
SOURCE
GATE
DRAIN
$Ga_{0.47}In_{0.53}As$
n+ CONTACT LAYER (5 nm)
$Al_{0.48}In_{0.52}As$
UNDOPED BARRIER LAYER (20 nm)
$Al_{0.48}In_{0.52}As$
n+ DONOR LAYER (12.5 nm)
$Al_{0.48}In_{0.52}As$
UNDOPED SPACER LAYER (2 nm)
$Ga_{0.47}In_{0.53}As$
UNDOPED CHANNEL (40 nm)
AlInAs/GaInAs
UNDOPED SUPERLATTICE
$Al_{0.48}In_{0.52}As$
UNDOPED BUFFER LAYER
InP
SEMI-INSULATING SUBSTRATE

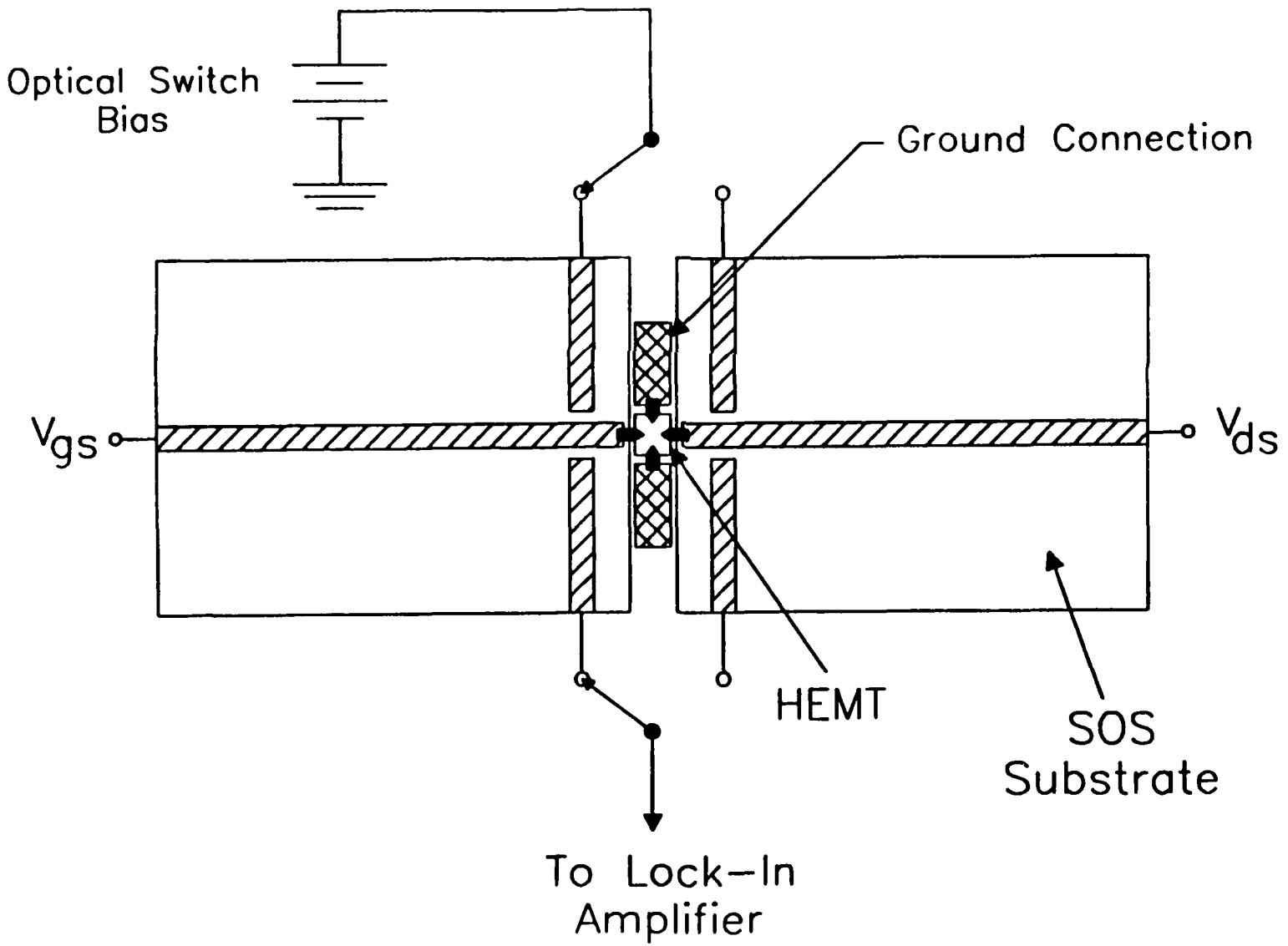
Optical Switch
Bias
Ground Connection
V_{gs}
V_{ds}
HEMT
SOS
Substrate
To Lock-In
Amplifier

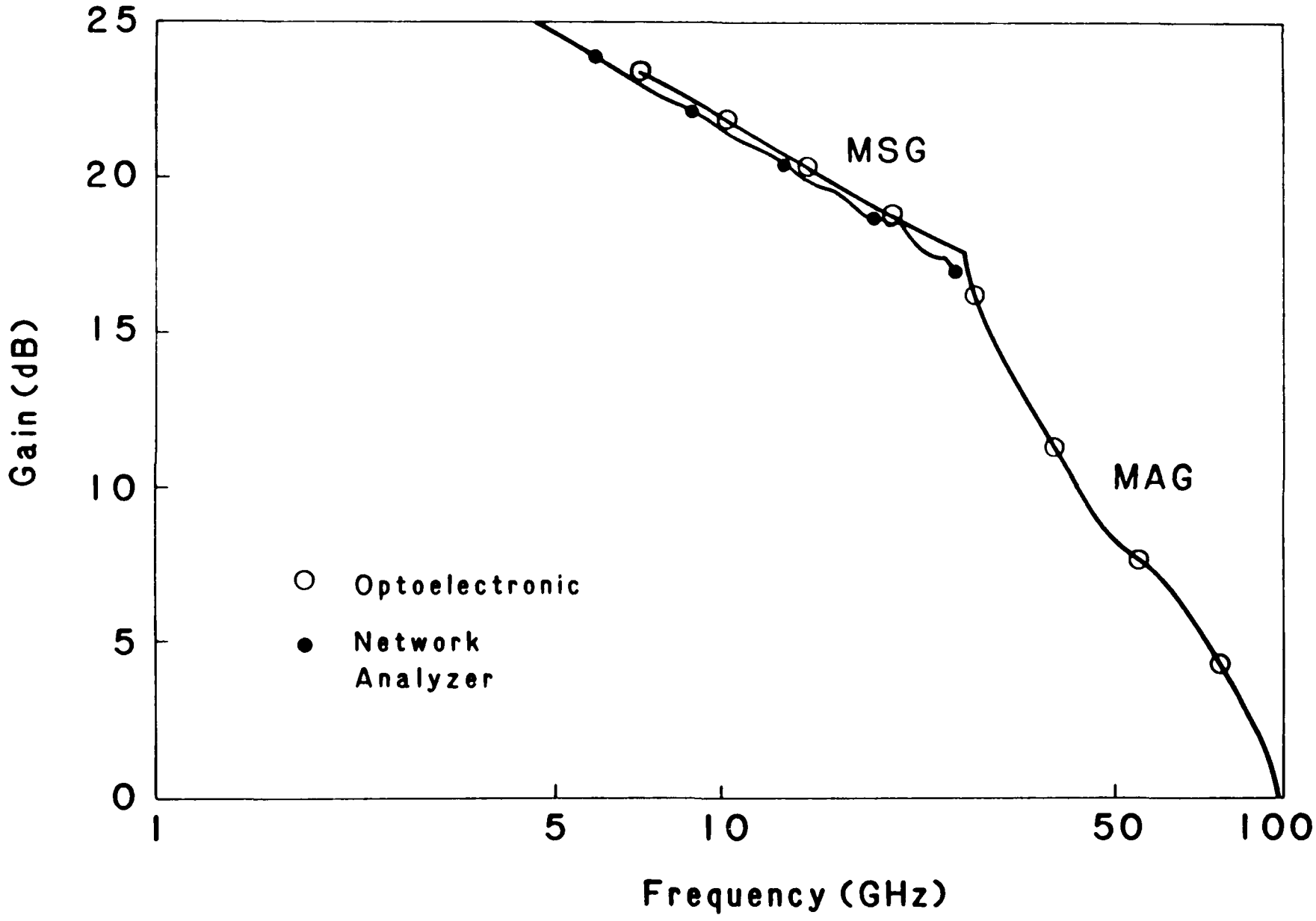
25
20
15
10
5
0
Gain (dB)
MSG
MAG
Optoelectronic
Network
Analyzer
1
5
10
50
100
Frequency (GHz)

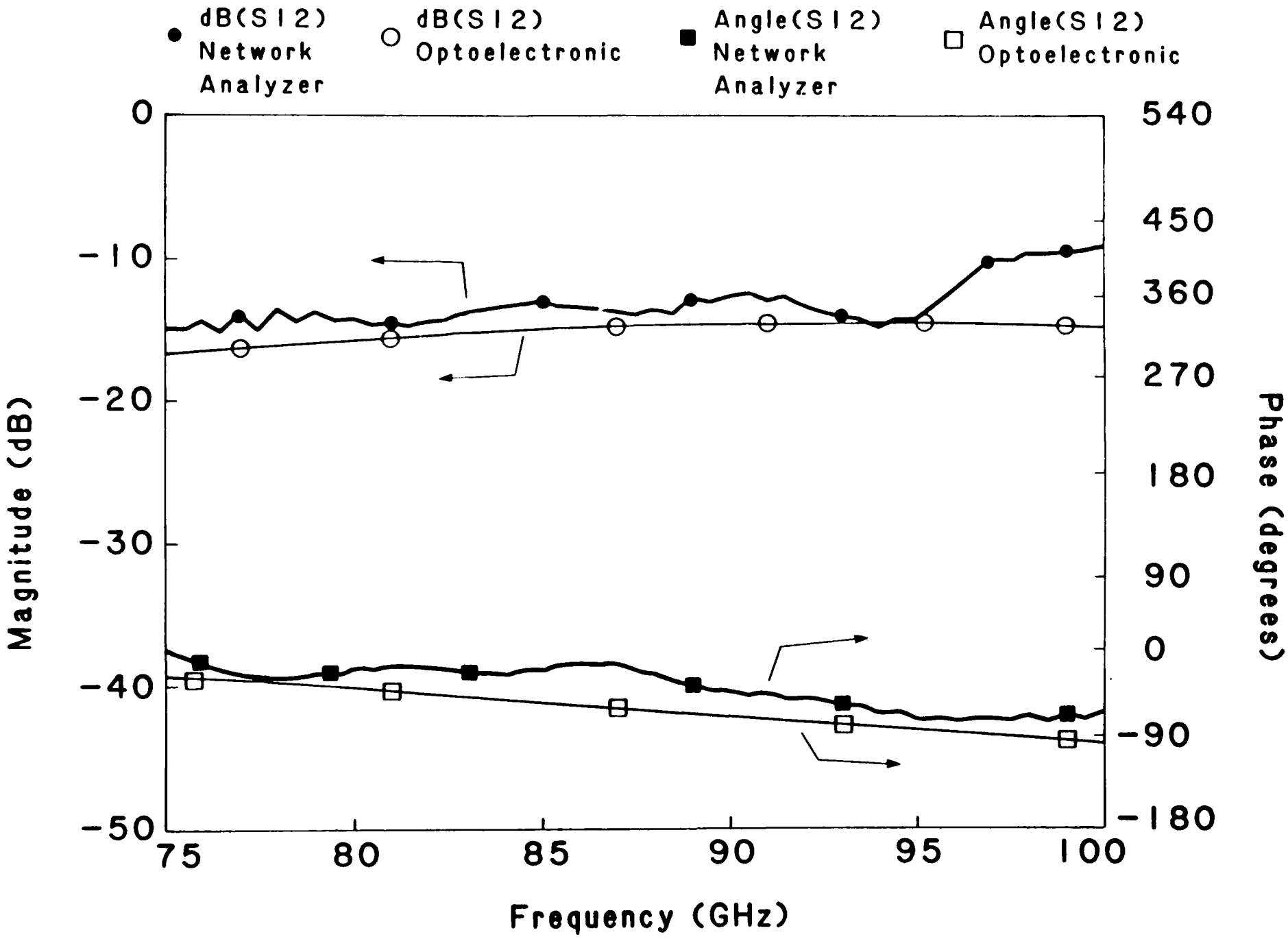
dB(S12) Network Analyzer
dB(S12) Optoelectronic
Angle(S12) Network Analyzer
Angle(S12) Optoelectronic
0
-10
-20
-30
-40
-50
540
450
360
270
180
90
0
-90
-180
75
80
85
90
95
100
Magnitude (dB)
Phase (degrees)
Frequency (GHz)

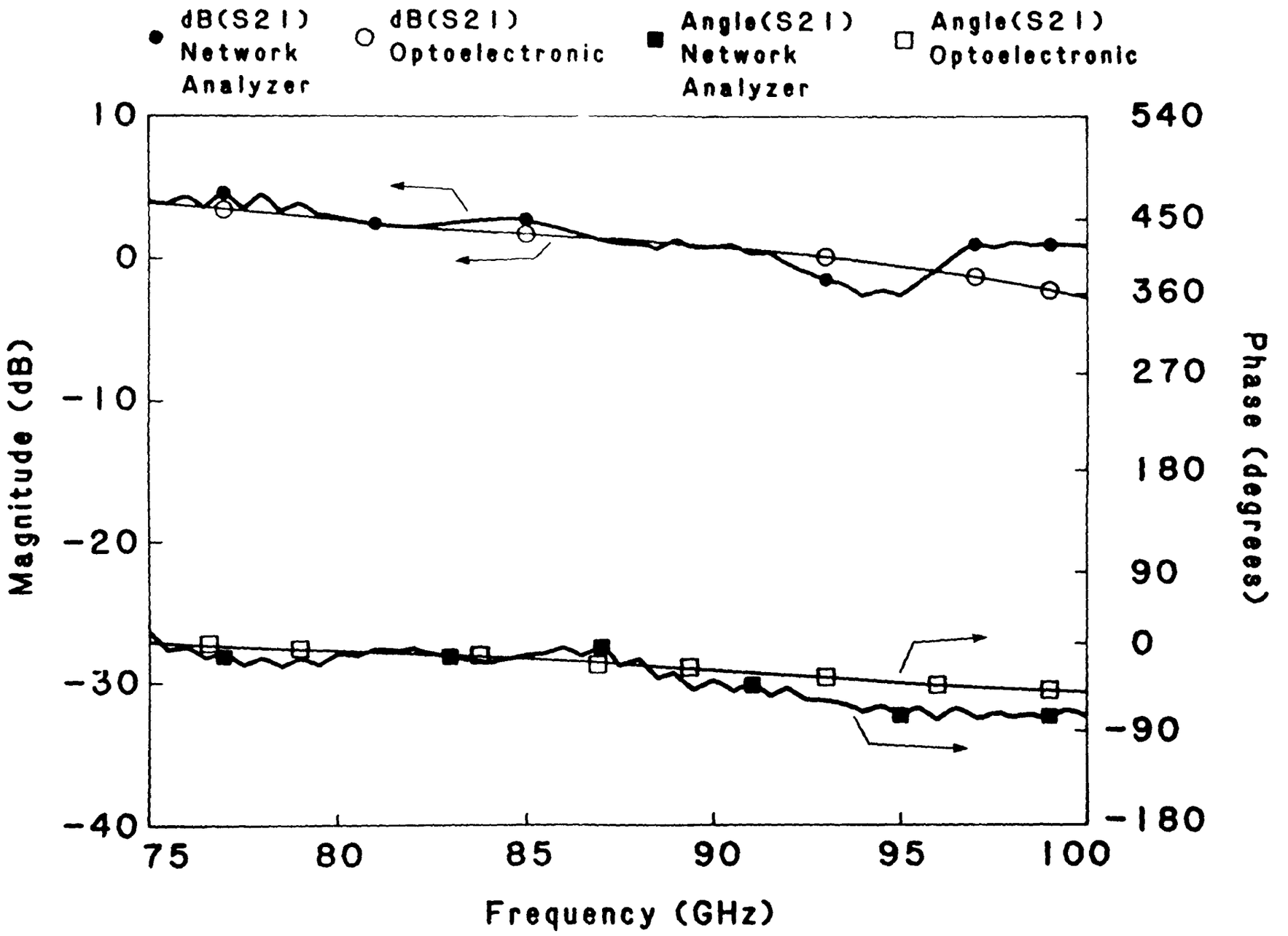
dB(S21) Network Analyzer
dB(S21) Optoelectronic
Angle(S21) Network Analyzer
Angle(S21) Optoelectronic
10
0
-10
-20
-30
-40
Magnitude (dB)
540
450
360
270
180
90
0
-90
-180
Phase (degrees)
75
80
85
90
95
100
Frequency (GHz)

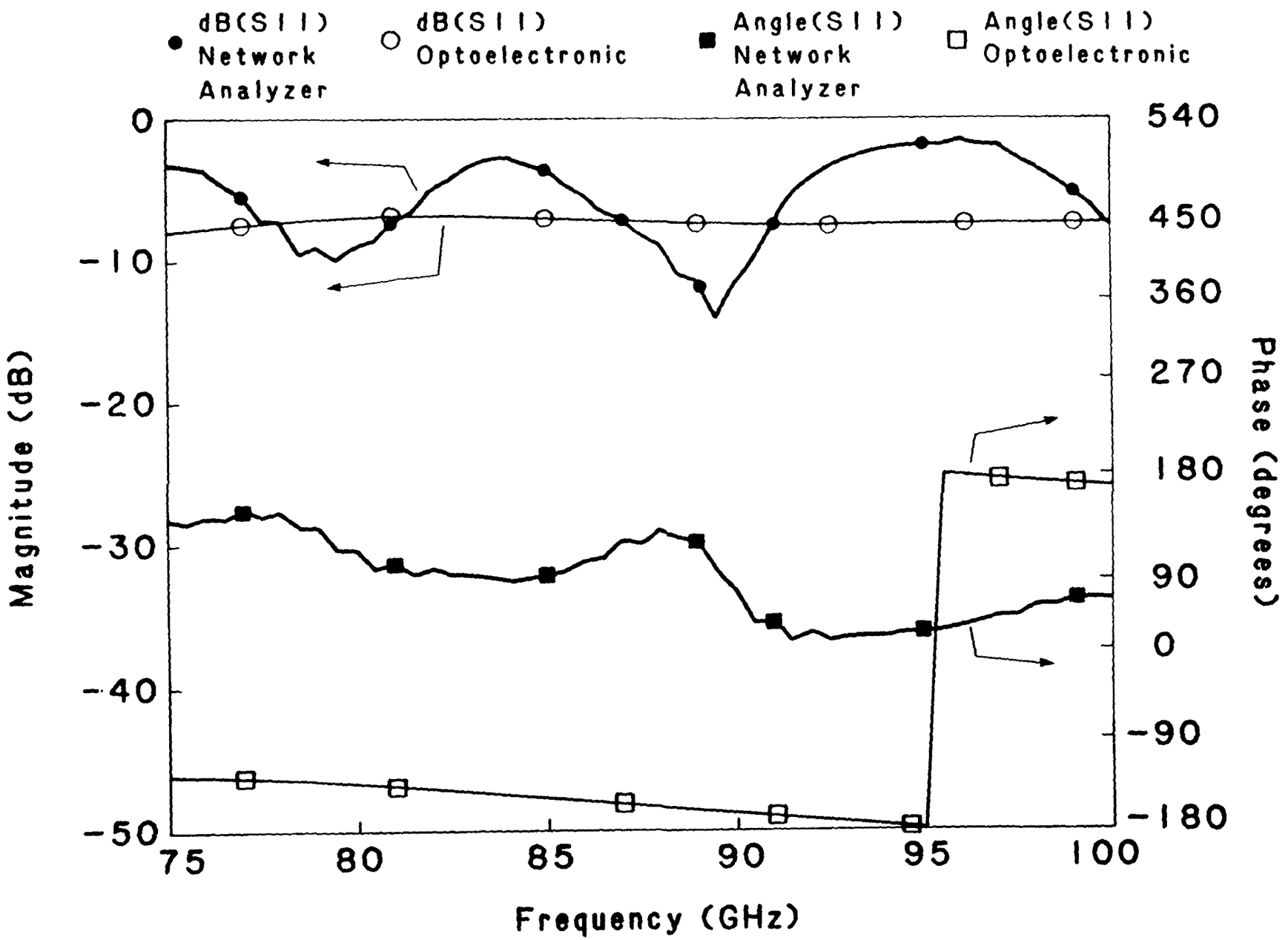
dB(S11) Network Analyzer
dB(S11) Optoelectronic
Angle(S11) Network Analyzer
Angle(S11) Optoelectronic
0
-10
-20
-30
-40
-50
Magnitude (dB)
540
450
360
270
180
90
0
-90
-180
Phase (degrees)
75
80
85
90
95
100
Frequency (GHz)

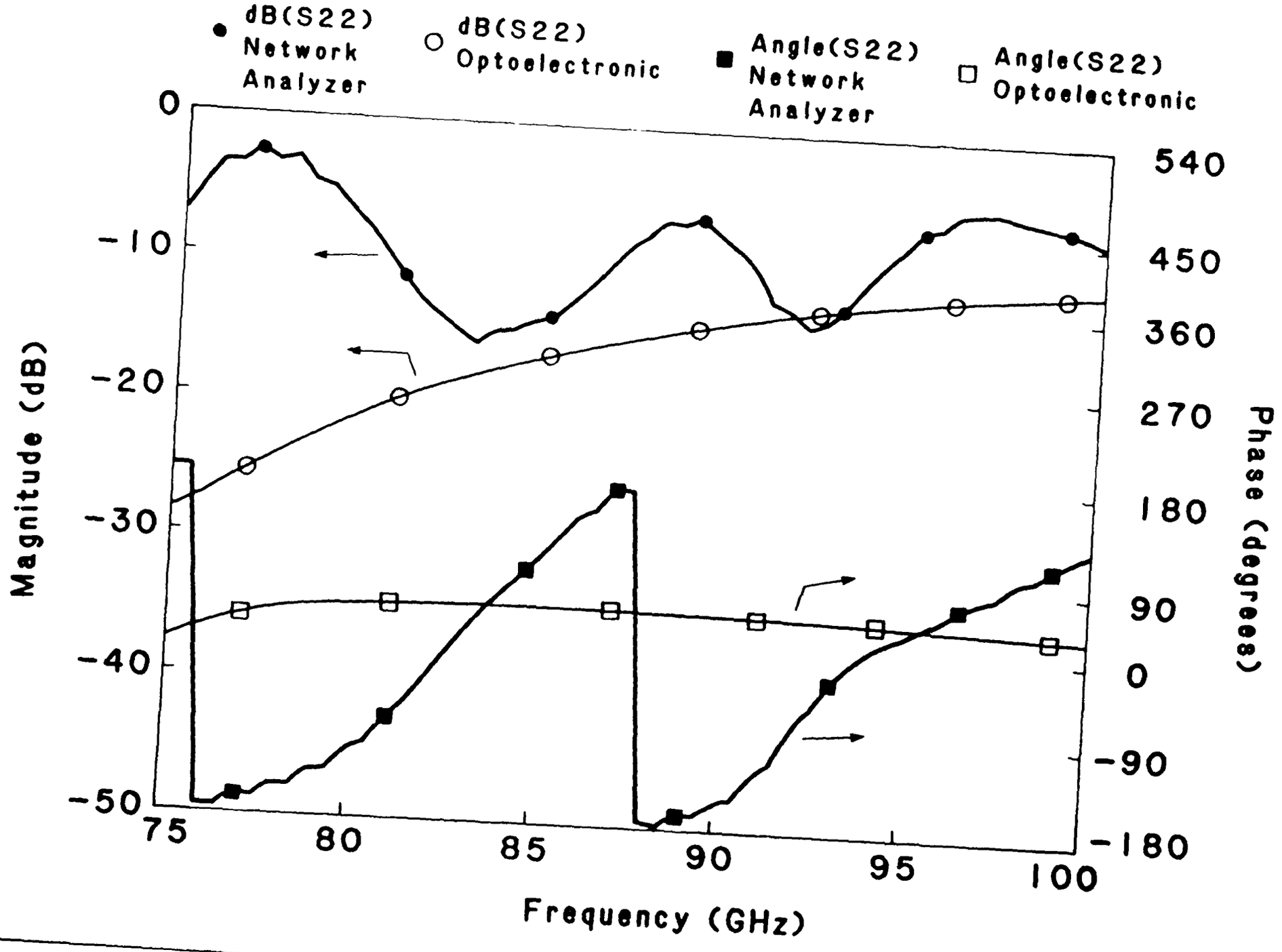
dB(S22) Network Analyzer
dB(S22) Optoelectronic
Angle(S22) Network Analyzer
Angle(S22) Optoelectronic
0
-10
-20
-30
-40
-50
Magnitude (dB)
540
450
360
270
180
90
0
-90
-180
Phase (degrees)
75
80
85
90
95
100
Frequency (GHz)

Use of Picosecond Optical Pulses and FETs Integrated with Printed Circuit Antennas to Generate Millimeter Wave Radiation

by

D.C. Ni., D.V. Plant, M. Matloubian, and H.R. Fetterman
Department of Electrical Engineering
University of California, Los Angeles
Los Angeles, California 90024

Millimeter wave radiation has been generated from FETs, integrated with printed circuit antennas, and illuminated with picosecond optical pulses. Sidebands on the millimeter waves were obtained by applying a swept RF modulation to the FET gate. Heterodyne detection and display demonstrates continuously tunable radiation, constrained by the high gain antenna, from 45 GHz to 75 GHz.

Recent experiments have shown that optoelectronic switches monolithically integrated with planar antenna structures can be used to generate electromagnetic radiation in the microwave and millimeter wave regions[1-11]. In these experiments, an optical pump and probe arrangement is used to coherently generate and sample the microwave and millimeter wave radiation. The bandwidth of these systems, when driven by picosecond optical pulses, extends from less than 10 GHz to greater than 200 GHz. These systems have been used in a number of applications including measuring the frequency dependent loss and dispersion properties of materials in the 10-130 GHz range, with a frequency resolution of 4.94 GHz[7,8,10,11]. Also, measurements of the transient far-field radiation properties of integrated optoelectronic antennas has provided both the temporal and spatial characteristics of these devices[9]. In addition, femtosecond optical pulses have been used to generate terahertz beams with bandwidth coverage from less than 100 GHz to greater than 2.0 THz[6,12,13,14].

Concurrently, optical control of millimeter wave devices has attracted recent attention because of its potential applications, such as enhanced device performance, signal switching, signal synchronization, and distributed control of communications and radar systems[15]. Techniques to study these effects include characterization of GaAs MESFETs, AlGaAs-GaAs HEMTs, and monolithic FET amplifiers by coherent optical mixing, and S-parameter and optical response measurements of similar devices using picosecond optoelectronic techniques [16,17,18,19]. Such studies have lead to an improved understanding of the photoconductive and photovoltaic mechanisms taking place in such devices under differing optical and electronic conditions.

In this letter, we report an alternative technique for generating millimeter waves which utilizes three terminal devices integrated with printed circuit antennas. This technique employs GaAs FETs, and related three terminal devices, mounted on printed circuit antennas and illuminated with picosecond optical pulses[20]. In addition, in an effort to increase the millimeter wave spectral coverage, a RF electrical modulation is applied to the gate of the transmitting device, and this modulation produces tunable sidebands on the millimeter wave radiation. Heterodyne detection rather than photoconductive sampling is used to measure the

radiation, and the measured signals are displayed in real time on a spectrum analyzer. The capabilities of this technique for high resolution real time millimeter wave spectroscopy are demonstrated by measuring the transmission response of a narrow bandwidth filter.

A schematic representation of the experimental arrangement is illustrated in figure 1. Similar planar twin dipole microstrip antennas with integrated FETs were used not only to transmit but also to receive the radiation. In the case of the transmitter, the drain and source of the FET were connected to the twin dipoles of the antenna, and in the case of the receiver, the gate and source were connected to the twin dipoles. Because the full characterization of the FETs integrated with the millimeter wave printed circuit antennas has been described elsewhere, a complete description will not be presented here[21].

In these most recent experiments, the active region of the transmitting FET was illuminated by 2.5 picosecond, 578nm optical pulses obtained from a synchronously pumped mode-locked Rhodamine 6G dye laser. The dye laser pump source was an actively mode-locked frequency doubled Nd:YAG laser operating at 76 MHz. The active region of the FET was excited by 50 to 150 milliwatts of average power focused to 5 μm in diameter with a 5X lens. In addition, using a sweep oscillator, a RF electrical modulation was applied to the transmitter gate. As is seen in the next section, this modulation produced tuneable sidebands on the millimeter waves. A klystron, tuneable from 55.5 GHz to 62.0 GHz, was used as a local oscillator for heterodyne detection of the radiation. The detected output was sent through various IF amplifiers (.75 - 2 GHz with a gain of 37 dB, and 6 - 18 GHz with a gain of 25 dB) and displayed in real time on a spectrum analyzer. Also, for purposes of data processing, a Hewlett-Packard 9836 computer was connected to the spectrum analyzer. Finally, two teflon lenses with 25.4 mm focal lengths were placed between the transmitter and the receiver to create a collimated beam into which a filter could be inserted.

The optical excitation produces a millimeter wave radiation comb whose signals are spaced 76 MHz apart. Because heterodyne detection is used, radiation products which fall within the bandwidth of the IF amplifier from both the high and the low frequency side of the local oscillator will be detected. This is seen in figure 2, where a spectrum

analyzer trace of the detected radiation for a local oscillator frequency of 61.4 GHz without transmitter gate modulation is shown. These data were taken using the .75 - 2 GHz IF amplifier and the devices biased as follows: the transmitting FET was biased with V_{ds} = 2.0V and V_{gs} = -3.0V, and the receiving FET was biased with V_{ds} = 2.0V and V_{gs} = -0.6V. By tuning the LO +/- 5.0 MHz the signals located in the upper sideband could be distinguished from those located in the lower sideband. In figure 2, the larger amplitude signals are in the upper sideband (61.52 GHz - 63.02 GHz) and the lower amplitude signals are in the lower sideband (59.78 GHz-61.28 GHz). Using various IF amplifiers, we found the bandwidth of the radiation comb extended from 45 GHz to 75 GHz, with each component spaced at 76 MHz. Also, using a wire grid polarizer, the beam was found to be linearly polarized, as was expected from antenna design considerations.

In an effort to further increase the frequency coverage, an electrical modulation was applied to the transmitter gate. This RF modulation produced tunable sidebands on the millimeter wave radiation. In order to demonstrate the capabilities of this system, we placed a Fabry-Perot interferometer with a narrow passband into the beam. The filter consisted of two 50 line/inch metal meshes mounted on optically flat retaining rings and separated using a translation stage. Figure 3a is a spectrum analyzer trace of the transmission response of this filter without gate modulation. The filter not only rejects the signals in the lower sideband (the lower amplitude signals in figure 2) but also rejects the signals in the upper sideband that are out of the passband of the filter. Applying a swept 100 Hz to 114 MHz, 0 dBm electrical modulation to the transmitting FET gate yielded a completely filled in transmission spectrum, as is shown in figure 3b. Here, the transmission response of the same filter is shown. The filter is tuned to approximately 62.27 GHz and has a FWHM of approximately 300 MHz, which is in good agreement with the calculated value. This figure shows the high spectral resolution obtainable with this technique.

Although in theory one need only apply a modulation from 100 Hz to 38 MHz to obtain complete frequency coverage, resonances occurring in the antenna circuit caused the ratio of the sideband power to carrier power to vary as a function of sideband frequency. Because of these resonances, the sideband modulation strength at certain frequencies was weak, and the resulting signal to noise was low. Attempts to apply a modulation

bandwidth of only 38 MHz, spaced at integer multiplies of 38 MHz (i.e. 38 - 76 MHz, or 76 - 114 MHz) yielded a similar lack of acceptable signal to noise. In order to most effectively trace out the response of the filter, the modulation bandwidth was extended to 114 MHz.

In conclusion, we have demonstrated an alternative technique for generating millimeter wave radiation utilizing active three terminal devices rather than passive two terminal switches. Although the frequency coverage is not as large as that of other techniques, the spectral resolution is very high. Signals are detected in real time thus eliminating the need for photoconductive sampling and Fourier transforming the detected transient radiation. Although mixing with the local oscillator fundamental frequency was used in this heterodyne detection scheme, detecting the millimeter wave radiation could also be accomplished using higher harmonics of a low frequency local oscillator. Signals can be superimposed on the gate of the receiving device antenna circuit at subharmonics of the desired local oscillator frequency, thus eliminating the need for a high frequency source.

As mentioned, the bandwidth of the radiation is limited primarily by the high gain antenna, and future improvements to this technique will include broadband, high frequency antennas integrated with high speed three terminal devices. Recently, work has been done to characterize some of the optical and electrical properties of FETs, HEMTs, and HBTs at frequencies in excess of 100 GHz, and these studies indicate such devices show excellent promise for use as these high frequencies[19,22]. Since a one picosecond optical pulse provides electrical bandwidths of greater than 100 GHz, integrating high speed three terminal devices with broadband antennas could potentially lead to complete frequency coverage from 10 GHz to greater than 100 GHz. In addition, cascading a number of devices to allow for signal amplification prior to driving the antenna, or tayloring the transmitting device construction and characteristics for improved signal strength will allow for improved performance and increased millimeter wave bandwidth.

This work was supported by the Air Force Office of Scientific Research. The authors would also like to thank Dr. Wilbert Chew for many helpful discussions.

References:

1) R. Heidemann, TH. Pfeiffer, and D. Jager, Electron. Lett. 19, 316 (1983).

2) D.H. Auston, K.P. Cheung, and P.R. Smith, Appl. Phys. Lett. 45, 284 (1984).

3) J.R. Karin, P.M. Downey, and R.J. Martin, IEEE J. Quantum. Electron. QE-22, 677 (1986).

4) A.P. DeFonzo, M. Jarwala, and C. Lutz, Appl. Phys. Lett. 50, 1155 (1987).

5) A.P. DeFonzo and C. Lutz, Appl. Phys. Lett. 51, 212 (1987).

6) P.R. Smith, D.H. Auston, and M.C. Nuss , IEEE J. Quantum. Electron. QE-24, 255 (1988).

7) Y. Pastol, G. Arjavalingam, J.-M. Halbout, and G.V. Kopcsay, Appl. Phys. Lett. 54, 307 (1989).

8) Y. Pastol, G. Arjavalingam, J.-M. Halbout, and G.V. Kopcsay, Electron. Lett. 25, 523 (1989).

9) C.R. Lutz and A.P. DeFonzo, Appl. Phys. Lett. 54, 2186 (1989).

10) Y. Pastol, G. Arjavalingam, G.V. Kopcsay, and J.-M. Halbout, Appl. Phys. Lett. 55, 2277 (1989).

11) G. Arjavalingam, Y. Pastol, J.-M. Halbout, and G.V. Kopcsay, IEEE Trans. Microwave Theory Tech. MTT-38, 615 (1990).

12) Ch. Fattinger and D. Grischkowsky, Appl. Phys. Lett. 53, 1480 (1988).

13) Ch. Fattinger and D. Grischkowsky, Appl. Phys. Lett. 54, 490 (1989).

14) Martin van Exter, Ch. Fattinger, and D. Grischkowsky, Appl. Phys. Lett. 55, 337 (1989).

15) R. Simons, *Optical Control of Microwave Devices*, Boston, Artech House, 1990, and references therein.

16) H. R. Fetterman, W.Y. Wu, and D. Ni., Proc. SPIE, vol. 789, 50, 1987.

17) H.R. Fetterman and D. Ni, Microwave Opt. Technol. Lett. 1, 34 (1988).

18) D.C. Ni, H.R. Fetterman, and W. Chew, IEEE Trans. Microwave Theory Tech. MTT-38, 608 (1990).

19) M. Matloubian, H.R. Fetterman, M. Kim, A. Oki, J. Camou, S. Moss, and D. Smith, IEEE Trans. Microwave Theory Tech. MTT-38, XXX (1990).

20) D.V. Plant, D.C. Ni, M. Matloubian, and H.R. Fetterman, Accepted for presentation at the IEEE/LEOS Annual Meeting, Boston, 1990.

21) W. Chew and H.R. Fetterman, IEEE Trans. Microwave Theory Tech. MTT-37, 593 (1989).

22) M. Matloubian, H.R. Fetterman, Submitted for publication.

Figure Captions:

Figure 1: Schematic of the experimental set-up. The optical beam was injected onto the device at an angle of 30 degrees with respect to the plane of the transmitting antenna, and the teflon lenses were separated by 10 cm.

Figure 2: Millimeter wave radiation comb produced by optical excitation for a local oscillator frequency of 61.4 GHz. Signals located in the upper sideband (61.52 GHz to 63.02 GHz) are the larger amplitude signals, and signals located in the lower sideband (59.78 GHz to 61.28 GHz) are the lower amplitude signals. The LO has been tuned such that the spacing between components in each of the two bands is 38 MHz.

Figure 3a: Transmission response of a metal mesh Fabry-Perot interferometer without transmitter gate modulation. The filter is tuned to 62.27 GHz, and the local oscillator is tuned to 61.4 GHz. The filter rejects not only signals in the lower sideband but also signals in the upper sideband that fall outside the passband of the filter.

Figure 3b: Transmission response of the same filter with a swept 100 Hz to 114 MHz, 0 dBm electrical modulation applied to the transmitting FET antenna circuit. This result demonstrates the high spectral resolution obtainable with this technique.

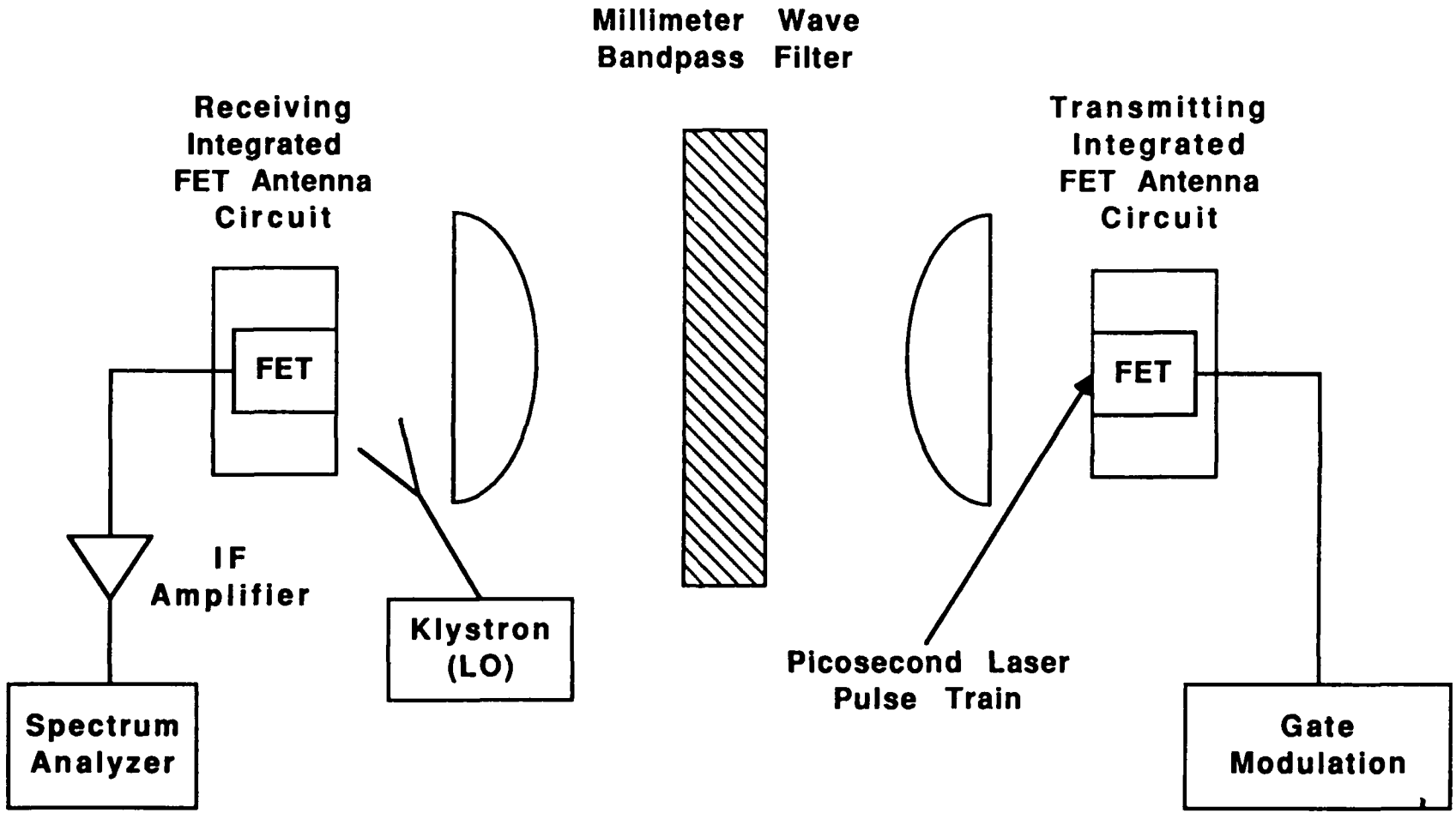
Millimeter Wave
Bandpass Filter
Receiving
Integrated
FET Antenna
Circuit
FET
IF
Amplifier
Klystron
(LO)
Spectrum
Analyzer
Transmitting
Integrated
FET Antenna
Circuit
FET
Picosecond Laser
Pulse Train
Gate
Modulation

FIGURE 1

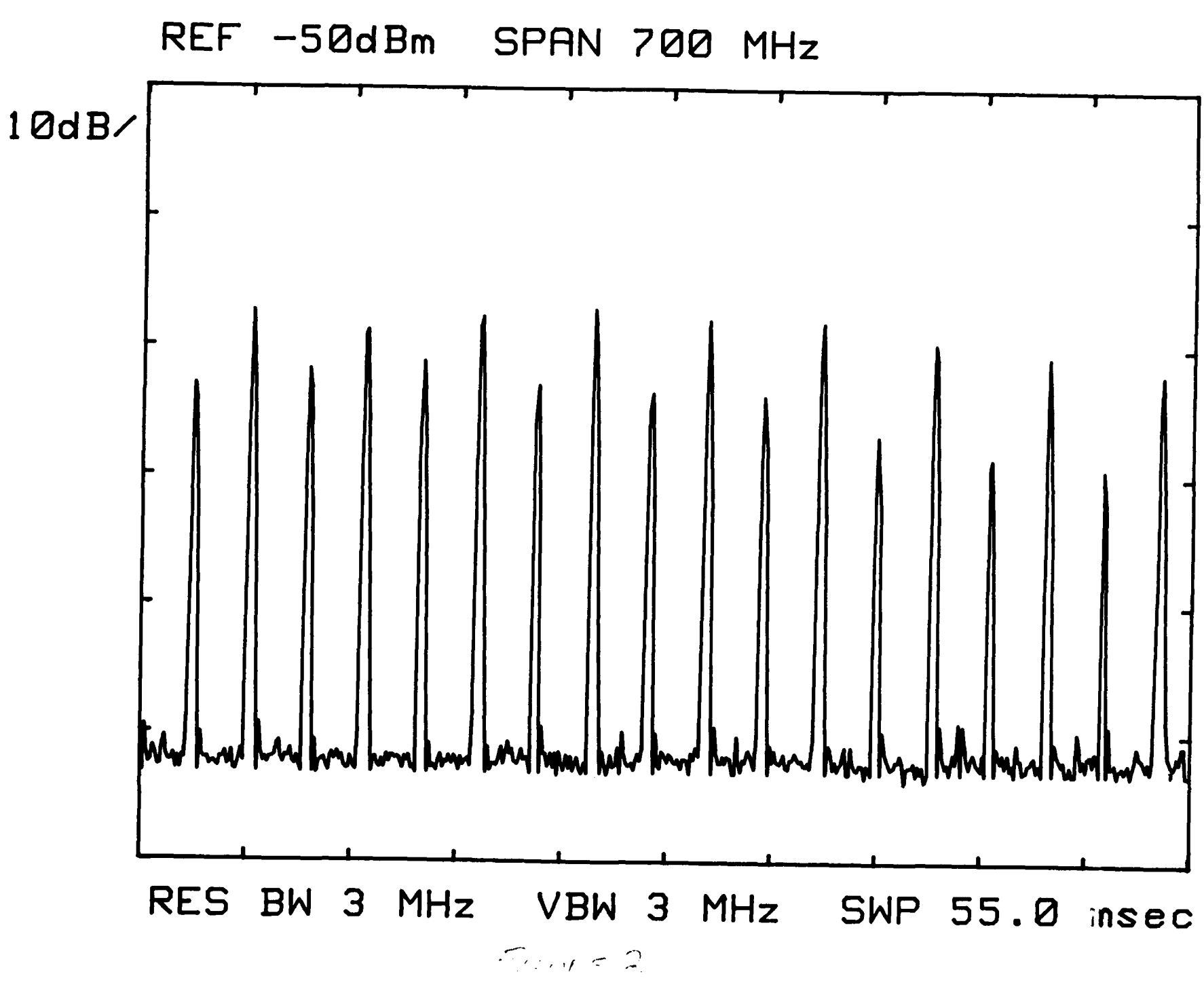
REF -50dBm SPAN 700 MHz
10dB/
RES BW 3 MHz VBW 3 MHz SWP 55.0 msec

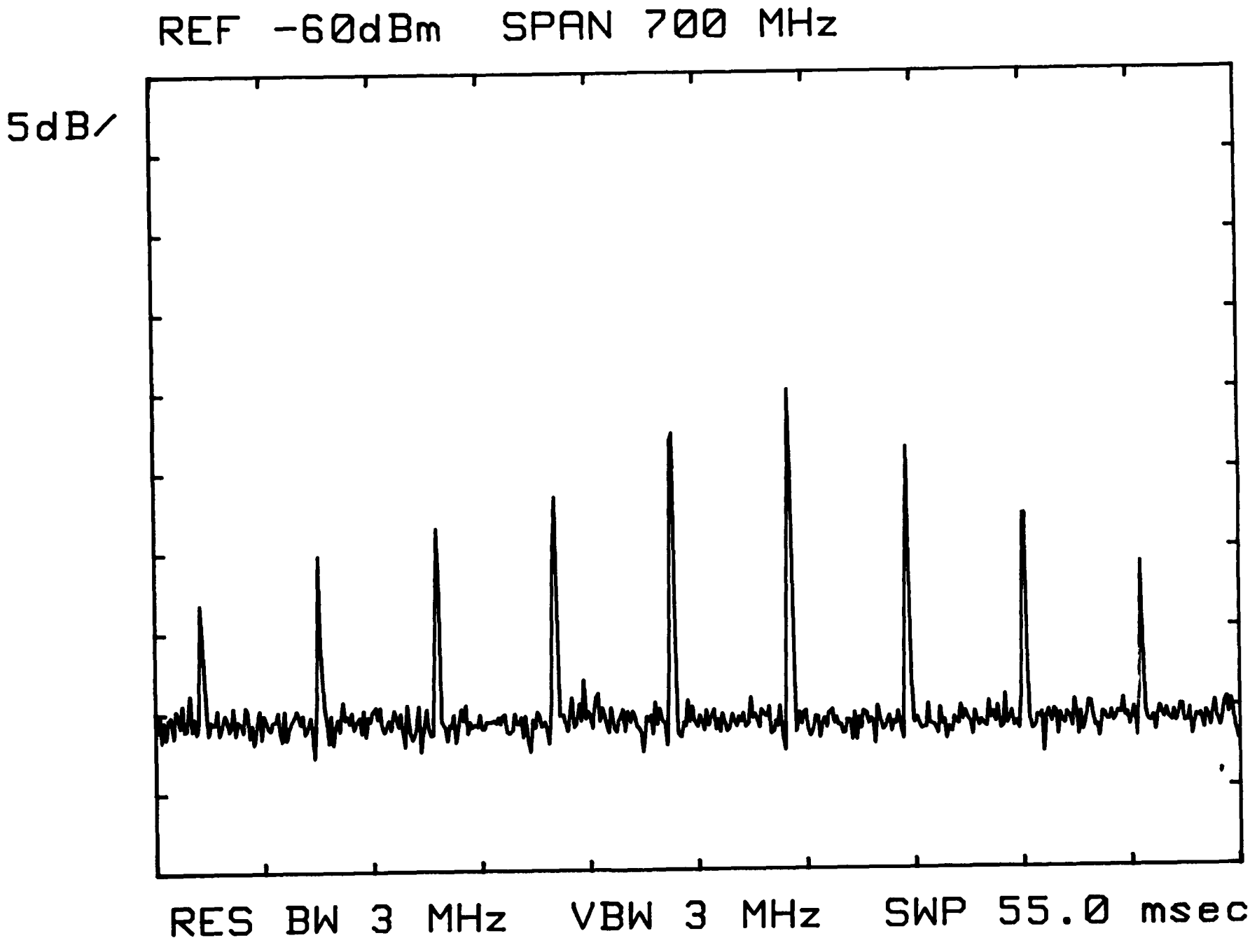
REF -60dBm SPAN 700 MHz
5dB/
RES BW 3 MHz VBW 3 MHz SWP 55.0 msec

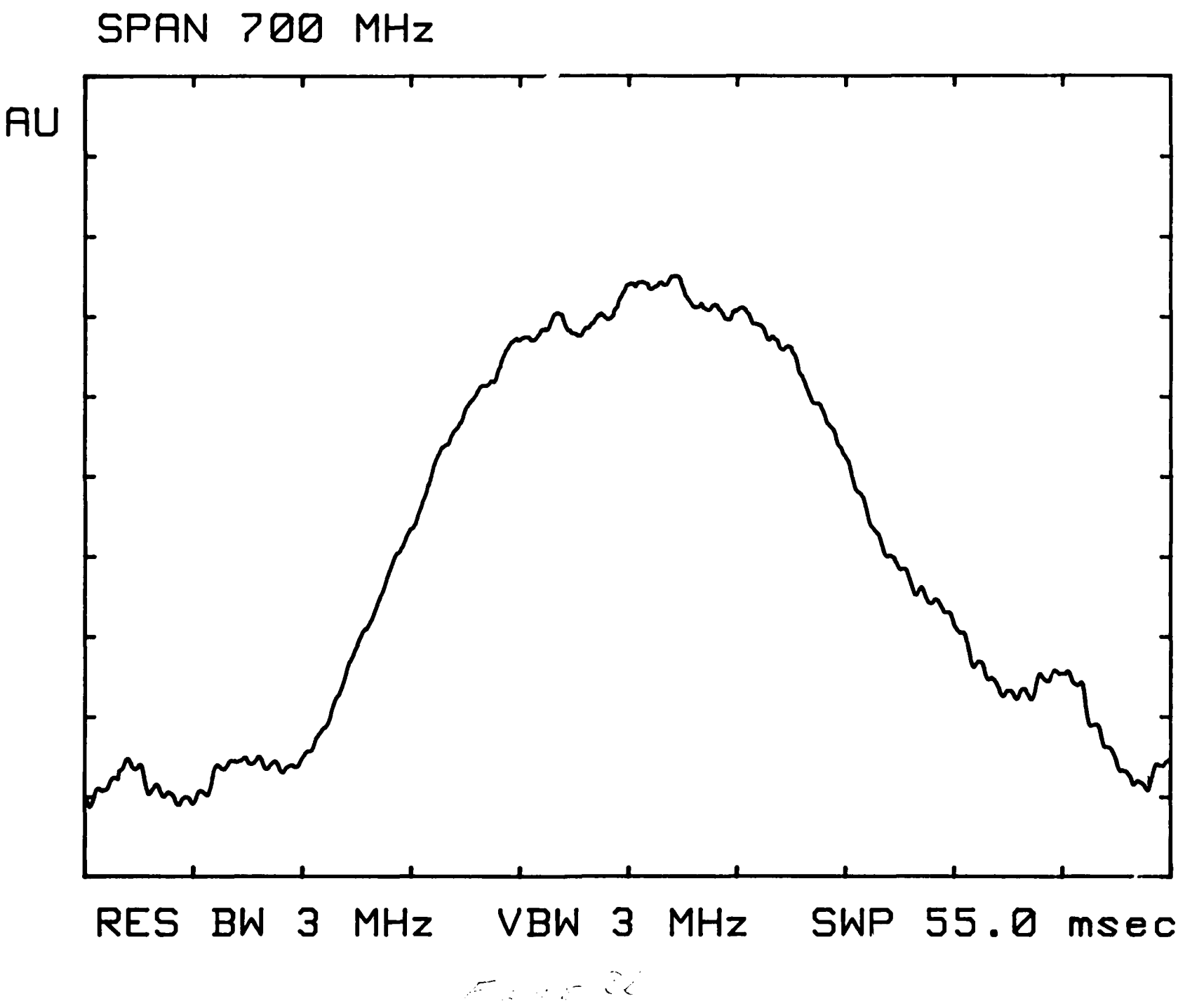
SPAN 700 MHz
AU
RES BW 3 MHz
VBW 3 MHz
SWP 55.0 msec